



OPEN ACCESS

EDITED BY

Laura Lorenzoni,
National Aeronautics and Space
Administration (NASA), United States

REVIEWED BY

Gerardo Toro-Farmer,
New College of Florida, United States
Elizabeth Wright-Fairbanks,
University Corporation for Atmospheric
Research (UCAR), United States

*CORRESPONDENCE

Constanza Ricaurte-Villota

✉ constanza.ricaurte@invemar.org.co

RECEIVED 02 October 2023

ACCEPTED 23 December 2024

PUBLISHED 30 January 2025

CITATION

Ricaurte-Villota C, Murcia-Riaño M and
Hernández-Ayón JM (2025) Dynamics and
drivers of the carbonate system: response to
terrestrial runoff and upwelling along the
Northeastern Colombian Caribbean coast.
Front. Mar. Sci. 11:1305542.
doi: 10.3389/fmars.2024.1305542

COPYRIGHT

© 2025 Ricaurte-Villota, Murcia-Riaño and
Hernández-Ayón. This is an open-access article
distributed under the terms of the [Creative
Commons Attribution License \(CC BY\)](https://creativecommons.org/licenses/by/4.0/). The
use, distribution or reproduction in other
forums is permitted, provided the original
author(s) and the copyright owner(s) are
credited and that the original publication in
this journal is cited, in accordance with
accepted academic practice. No use,
distribution or reproduction is permitted
which does not comply with these terms.

Dynamics and drivers of the carbonate system: response to terrestrial runoff and upwelling along the Northeastern Colombian Caribbean coast

Constanza Ricaurte-Villota ^{1*}, Magnolia Murcia-Riaño ¹
and José Martín Hernández-Ayón ²

¹Marine and Coastal Geosciences Program, Marine and Coastal Research Institute "José Benito Vives de Andrés" (INVEMAR), Santa Marta, Colombia, ²Instituto de Investigaciones Oceanológicas, Universidad Autónoma de Baja California, Ensenada, Mexico

Introduction: This study investigated the variability and main drivers of the carbonate system in Gayraca Bay and Chengue Bay, located on the northeastern Caribbean coast of Colombia, through monthly measurements of partial pressure of CO₂ (pCO₂), pH, total alkalinity (TA), and dissolved inorganic carbon (DIC) from 2017 to 2022. Statistical analyses and Taylor series decomposition were employed to determine the seasonal and interannual contributions of sea surface temperature, salinity, TA, and DIC to changes in pCO₂, pH, and calcium carbonate saturation state (Ω).

Results: The results showed significant seasonal variability influenced by annual changes in coastal upwelling, rainfall, and river runoff. Low/high pH and Ω values were associated with high/low DIC and TA values during the dry and wet seasons, respectively, while pCO₂ exhibited an opposite pattern. During El Niño, negative anomalies in coastal upwelling produced negative anomalies in pCO₂ and positive anomalies in Ω , DIC, and TA. Conversely, during La Niña, alternating periods of positive rainfall and upwelling anomalies were observed. Higher rainfall corresponded to negative anomalies in pCO₂, DIC, and TA and positive anomalies in Ω , whereas stronger upwelling led to opposite trends. In early 2022, undersaturated levels of Ω_{calc} and Ω_{arag} (<1) were observed, which could affect coral calcification and pose risks in future climate change scenarios. Taylor series decomposition analysis identified TA and DIC as primary drivers of carbonate system variability, modulated by seasonal and interannual changes in rainfall and river runoff, which are influenced by ENSO events. The observed trends in pH and pCO₂ were driven by a decrease in DIC and TA, attributed to increased river runoff, contrasting with typical ocean acidification trends driven by rising atmospheric CO₂ levels.

Discussion: This highlights the region's unique dynamics and underscores the importance of local studies. This study provides a novel 6-year time-series dataset for the carbonate system in the Colombian Caribbean, offering a valuable baseline for assessing the impacts of global warming and ocean acidification in the region.

KEYWORDS

ocean acidification, upwelling, tropical oceans, coral reef areas, Caribbean surface water, subtropical subsurface water, riverine input, ENSO

1 Introduction

Ocean acidification (OA), a reduction in pH caused by the absorption of atmospheric CO₂, alters the carbonate balance (Feely et al., 2004; Orr et al., 2005; Fabry et al., 2008; Doney et al., 2009a). Rising water temperatures and OA threaten the long-term health of calcifying organisms and the persistence of coral reef ecosystems (Silverman et al., 2009). In coastal zones and shallow environments, OA is exacerbated by highly variable coastal processes influenced by multiple factors, including freshwater and nutrient inputs, biological processes, and upwelling (Doney et al., 2009a; Rheuban et al., 2019; Cai et al., 2021; Wright-Fairbanks and Saba, 2022). Despite their importance, the impacts of these factors have been poorly studied in tropical areas, especially in Latin America. Furthermore, the magnitude of the sinks and the degree of acidification in marine shelf areas are not accurately known, mainly due to limited time series and higher natural spatiotemporal variability compared to that of open ocean systems (Omar et al., 2019).

Carbonate chemistry variability in tropical areas caused by seasonal upwelling has been observed in the Gulf of Papagayo (Sánchez-Noguera et al., 2018), Gulf of Tehuantepec (Chapa-Balcorta et al., 2015), and Galapagos Islands (Manzello et al., 2014). However, little is known regarding how regional upwelling affects the variability of the carbonate system in these important regions or the Caribbean. Indeed, few Latin American countries with tropical coastal zones have produced robust time series with high-quality data on carbonate system variables, although Mexico (Hernández-Ayón et al., 2003, 2013; Norzagaray-López et al., 2013, 2015, 2017; Chapa-Balcorta et al., 2015), Costa Rica (Sánchez-Noguera et al., 2018), and Brazil (Parard et al., 2010; Valerio et al., 2021) are notable exceptions, and modeling information is available for the region (Takahashi et al., 2002; Doney et al., 2009b; Gallego et al., 2018; Gregor and Gruber, 2021).

In the northern Caribbean, a 17-year dataset was generated with ships of opportunity, which has been used to evaluate decadal trends and patterns of the inorganic carbon cycle and OA (Wanninkhof et al., 2020). Gledhill et al. (2008) compiled satellite data, modeling results, and measurements from ships of opportunity and geochemical prospecting efforts in the Greater Caribbean region, such as those conducted within the World Ocean Circulation Experiment program (WOCE 22 and AR01) and Eastern Boundary Current cruise (ABACO). Woosley et al. (2016) evaluated a transect in the western Atlantic (centered at 66° W, between 11° and 40° N) to analyze anthropogenic carbon capture and storage. Astor et al., 2005, 2013) examined the variability of DIC and CO₂ fugacity (fCO₂) in the Cariaco Basin, off Venezuela. Tigreros (2013) studied the north-central Colombian Caribbean Sea, reporting that the average partial pressure of CO₂ (pCO₂-sea) was greater than the atmospheric partial pressure of CO₂ (pCO₂-atm). Given this difference, the system attains equilibrium by releasing CO₂ into the atmosphere. Despite these advances, uncertainty still surrounds the carbonate system in the Caribbean region.

The Tayrona National Natural Park (TNNP) is located within the Southern Caribbean Upwelling System (Correa-Ramirez et al., 2020), which covers the northern part of Colombia and Venezuela. Upwelling and terrestrial runoff converge in the TNNP, resulting in seasonal and interannual variability (Bayraktarov et al., 2014). During the upwelling season, the region acts as a source of CO₂ to the atmosphere (Astor et al., 2005). Interannual variability in pCO₂ is positively related to sea surface temperature (SST), and low but significant correlations between SST and the Atlantic Multi-decadal Oscillation (AMO) and El Niño Southern Oscillation (ENSO) have also been identified (Astor et al., 2013). The TNNP is representative of the biodiversity of the coral formations in Colombia and provides habitats for many fish species and benthic organisms.

Carbonate system drivers have been investigated worldwide (Lovenduski et al., 2007; Doney et al., 2009b; Gallego et al., 2018; Gregor and Gruber, 2021). Although multiple studies have investigated these drivers in temperate regions (Rheuban et al., 2019; Da et al., 2021; Wright-Fairbanks and Saba, 2022), the drivers behind the seasonal cycle and interannual variability have not been documented in tropical zones, such as the Caribbean, where the sea theoretically behaves as a CO₂ source (Takahashi et al., 2002). Thus, this study aimed to understand the spatiotemporal variation of the carbonate system in the TNNP, including the effects of local (river runoff and seasonal upwelling) and regional (ENSO) drivers. This survey provides a novel dataset (2017–2022) composed of monthly data on the carbonate system and meteorological, hydrological, and oceanographic variables for the northeastern Colombian Caribbean, thus establishing a baseline to study the effects of global warming in the region.

2 Methodology

2.1 Study area

This study was conducted in the Gayraca and Chengue Bays of the TNNP (Figure 1), located within a coastal complex formed by the entrance of the sea in the northwestern Sierra Nevada de Santa Marta (Garzón-Ferreira et al., 2004). The continental shelf of the TNNP is narrow, with depths of 200 m within 2 km from the coast. The TNNP is a biodiversity hotspot in the Caribbean, hosting 500–1000 benthic species, including mollusks, echinoderms, corals, and sponges (Miloslavich et al., 2010), as well as coral communities, seagrass meadows, and mangrove ecosystems in its capes, inlets, and bays (Bayraktarov and Wild, 2014). The western sides of the bays are more exposed to wave action, with the more protected eastern areas hosting complex and species-rich coral formations dominated by massive colonies (Díaz et al., 2000). Coral and crustose coralline algae coverage is higher in the exposed areas of the bays than in the protected areas (Eidens et al., 2014).

From December to April (boreal winter) and July to August (known as *Veranillo de San Juan*), periods of low precipitation and trade wind intensification occur in the TNNP

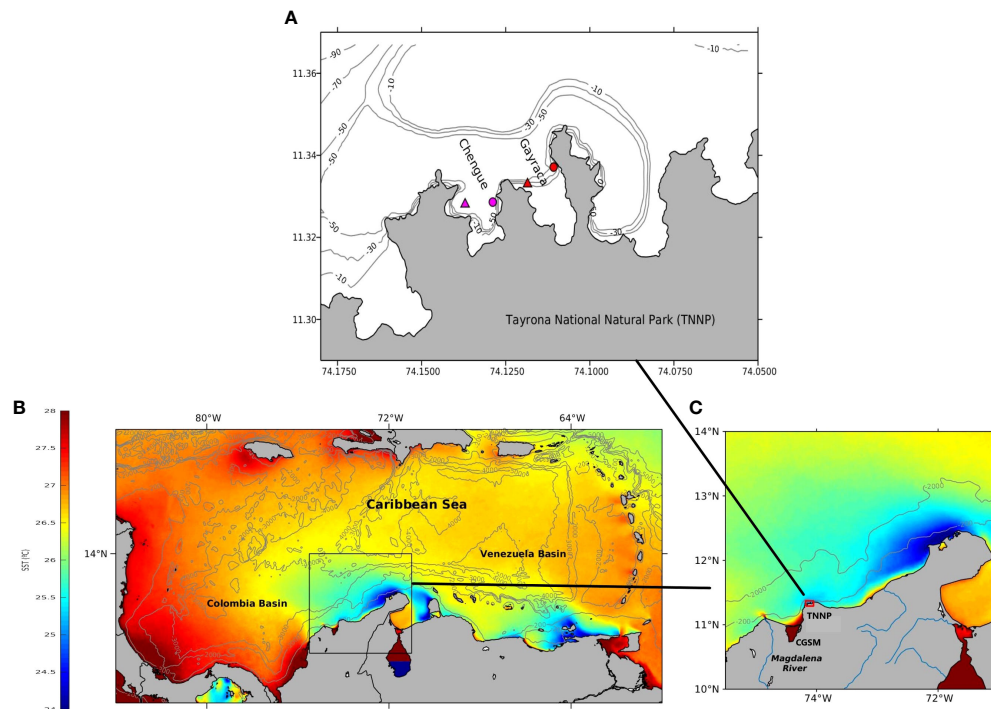


FIGURE 1

Map with bathymetric contours of the Gayraca and Chengue Bays in the Tayrona National Natural Park (TNNP). Triangles represent exposed areas, while circles indicate sheltered areas (A). Climatological average of the sea surface temperature (SST, °C) for the Caribbean Sea in February (17 years, 2003–2019) (B). The black box shows the location of the study area in the continental Colombian Caribbean (northeastern Caribbean Coast of Colombia). The red box indicates the location of the TNNP (C). The temperatures of the waters influenced by the Magdalena River and the Ciénaga Grande de Santa Marta are also shown.

(Salzwedel and Müller, 1983; Diaz-Pulido and Garzón-ferreira, 2002; Sarmiento-Devia et al., 2013; Correa-Ramirez et al., 2020). Wind intensification results in La Guajira upwelling, which forms part of the western South Caribbean Upwelling System (Figure 1B). In the southeastern Caribbean, La Guajira upwelling raises cold subsurface waters (average of 24–25.5°C; Correa-Ramirez et al., 2020) belonging to Subtropical Underwater (SUW) with distinct biogeochemistry (Cervantes-Díaz et al., 2022) from those of the surrounding Caribbean surface waters (average temperature of 26.5–28°C). A minor rainy season and weakened winds are present from May to June (Sarmiento-Devia et al., 2013). The highest precipitation due to the migration of the Intertropical Convergence Zone (ITCZ) occurs from September to November. This migration also alters wind intensity and intensifies terrestrial runoff (Bayraktarov et al., 2014).

The mouth of the Magdalena River (Bocas de Ceniza and Boca de la Ciénaga Grande de Santa Marta; Figure 1C) is located in the southwestern region of the study area. The Magdalena River extends 1613 km, and its drainage basin covers 257,438 km². The Magdalena River flows northward through Colombia and discharges into the Caribbean Sea (annual discharge of 228 km³). According to data from the Calamar station (112 km upstream), the average annual flow rate of Magdalena River discharge is 7200 m³·s⁻¹, with low average discharge (4068 m³·s⁻¹) in March and high average discharge (10287 m³·s⁻¹) in November (Restrepo and Kjerfve, 2000). ENSO

affects the rainfall regime in the Colombian Andes (Poveda and Mesa, 1997), where the Magdalena River originates, and is strongly associated with the interannual variability of Magdalena River discharge. Precipitation increases when negative Oceanic Niño Index (ONI) anomalies are recorded in the Pacific Ocean (cold phase-La Niña), resulting in increased flow (Poveda and Mesa, 1996). When positive ONI anomalies are recorded (warm phase-El Niño), precipitation decreases, negatively affecting flow rates. The ENSO phenomenon explains up to 65% of the interannual variability in the flows of the main rivers in Colombia that discharge into the Caribbean Sea (Restrepo and Kjerfve, 2000; Gutiérrez and Dracup, 2001). The flow rates associated with negative ONI anomalies of the La Niña phase exceed 12000 m³·s⁻¹, whereas the flow rates associated with the positive ONI anomalies of the El Niño phase range from 2000 to 3000 m³·s⁻¹ (Restrepo and Kjerfve, 2000).

In addition to the Magdalena River (which enters this swampy complex through channels on the western side), the Fundación, Aracataca, and Sevilla Rivers descend from the Sierra Nevada de Santa Marta and discharge in the southern and eastern sides of the Ciénaga Grande de Santa Marta lagoon. The flow through the mouth of the Ciénaga Grande de Santa Marta, called Boca de la Barra, ranges from 200 to 700 m³·s⁻¹ throughout the year (Ricaurte-Villota et al., 2018). The contributions of continental water and those from the Magdalena River primarily reach the study area during the intense rainy season from September to November,

when the northeast trade winds weaken and the coastal counter-current strengthens (Pujos et al., 1986). Romero-Rodríguez et al. (2017) also noted these patterns in the climatology of the Magdalena River sediment plume extension in data from the MODIS sensor (555-nm band).

2.2 Data collection and processing

To assess the spatiotemporal variation of the carbonate system in the TNNP related to climatic and oceanographic forcings, measurement stations were established in the exposed and protected areas of the Gayraca and Chengue Bays (Figure 1C). Field measurements were taken monthly between March and November 2017, January and November 2018, March and December 2019, February 2020 (due to the COVID-19 pandemic), October and December 2020, March and December 2021, and January and October 2022 and complemented with satellite and ONI data.

2.2.1 Climatic and oceanographic forcing

To assess the forcings that influence the variability of the carbonate system in the study area, we analyzed monthly meteorological (wind and precipitation), hydrological (Magdalena River flow rates), and oceanographic (SST, salinity, and dissolved oxygen) data. Wind speed data from a point near the study area (11° 30' N, 74° 15' W), which were also used to calculate the upwelling index and monthly climatological analysis, were obtained from the fifth-generation ERA-5 reanalysis dataset (Hersbach et al., 2023) available on the Copernicus platform; these data have a spatial resolution of 0.25° x 0.25° and an hourly temporal resolution.

We calculated the upwelling index, which considers the volume of water transported per unit of time and distance along the coast, to determine the contribution of upwelled water to the study area. We followed the methodology of Bakun (1973) and calculated Ekman transport as follows (Equation 1):

$$Q_x = \frac{\tau_y}{\rho f} (10^3) \quad Q_y = \frac{-\tau_x}{\rho f} (10^3) \quad (1)$$

where ρ is the air density ($\rho = 1.2 \text{ kg}\cdot\text{m}^{-3}$), f is the Coriolis parameter (f), and $\tau_y - \tau_x$ are the wind stress components calculated via the wind speed for each west-east (Q_y) and north-south (Q_x) component (Equation 2). Monthly ERA-5 wind data were used.

$$T_x = \rho_a C_d \sqrt{u^2 + v^2} \mu \quad T_y = \rho_a C_d \sqrt{u^2 + v^2} v \quad (2)$$

where $\rho_a = 1025 \text{ kg}\cdot\text{m}^{-3}$ is the water density and C_d is the drag coefficient ($C_d = 1.4 \times 10^{-3}$). Based on the results obtained for the zonal and meridional Ekman transport (Q_x and Q_y), the upwelling index was calculated for each month (2017–2022; Equation 3):

$$UI = -\sin(\theta)Q_x + \cos(\theta)Q_y \quad (3)$$

theta (θ) is the mean angle between the shoreline and the equator (37.82°).

The rainfall data for the study period were obtained from the Institute of Hydrology, Meteorology, and Environmental Studies (IDEAM)¹ Aeropuerto Simón Bolívar station. The monthly flow rates of the Magdalena River and its monthly climatological patterns, which were used as an indicator of terrestrial runoff, were calculated from the 2007–2022 time series of the IDEAM² Calamar station.

The annual SST cycle was derived from a 15-year time series (2007–2022) of the Global Ocean OSTIA Sea Surface Temperature and Sea Ice Analysis product (Good et al., 2020) obtained from the Copernicus Marine Service (CMEMS)², with a spatial resolution of 1/20° (~6 km) and daily temporal resolution. The annual sea surface salinity (SSS) cycle for 2007–2022 was obtained from the Global Ocean Physics Reanalysis and Global Ocean Physics Analysis and Forecast products, also available from the Copernicus Marine Service platform. This reanalysis had a spatial resolution of 1/12° (~9 km) and daily temporal resolution.

To analyze temperature, salinity, and dissolved oxygen from 2018 onward, we used *in situ* measurements from a CTD system (Conductivity, Temperature, Depth) composed of a CTD SBE 19Vplus unit (Sea-Bird Scientific, Bellevue, USA) equipped with sensors for pressure (SBE-19P, initial accuracy $\pm 0.1\%$ of full-scale range), temperature (SBE19plusV2, initial accuracy $\pm 0.005^\circ\text{C}$), conductivity (SeaCAT Profiler, initial accuracy $\pm 0.0005 \text{ S/m}$), and dissolved oxygen (SBE-43, initial accuracy $\pm 2\%$ of saturation). These sensors were calibrated at SBE headquarters on multiple occasions: November 2014, July 2017, December 2018, and September 2019. The CTD data were post-processed according to standard practices using Sea-Bird Data Processing software³. From temperature and salinity data throughout the water column, we identified the water masses in the study area during different climatic seasons by plotting potential temperature against absolute salinity (Θ -SA diagram), following the classifications proposed by Emery and Meincke (1986); Giraldo (1994), and Hernandez-Guerra and Joyce (2000). Dissolved oxygen was used as a water mass tracer.

To evaluate interannual changes related to ENSO, we used ONI⁴ data from 2017 to 2022 and compared them with the deseasonalized standardized anomalies of carbonate system variables for the exposed Gayraca site. Spearman correlations (95% confidence) between the ONI and carbonate system variable anomalies were calculated using Minitab v. 21.1.0.

2.2.2 Carbon biogeochemistry and saturation state in the Tayrona National Natural Park

To study carbonate biogeochemistry, pH profiles (NBS scale) from the surface to approximately 20 m were generated from the data collected with the CTD fitted with a pH sensor (SBE-18, $\pm 0.1 \text{ pH}$ stated accuracy achievable with frequent field calibrations). The on-site sensor calibration followed the no. 18-1⁵ application note for SBE

1 <http://dhime.ideam.gov.co/atencionciudadano/>

2 <https://marine.copernicus.eu/>

3 <https://www.seabird.com/software>

4 https://origin.cpc.ncep.noaa.gov/products/analysis_monitoring/ensostuff/ONI_v5.php

18, using three standard pH buffer solutions (pH 4.01, 7.00, and 10.00) provided by WTW, a division of Thermo Fisher Scientific. This sensor was also calibrated at the SBE main facility in March 2017, July 2017, and December 2018. The NBS scale was utilized as the CTD, and its calibration solutions are standardized for this scale.

Water samples were collected from the surface layer at each station using 5-L Niskin bottles to measure pH, dissolved inorganic carbon (DIC), and total alkalinity (TA) in the laboratory. Each sample was transferred to a 40-ml amber borosilicate bottle with double septa and fixed with 10 µl (i.e., the minimum recommended amount) of mercury chloride (HgCl₂) solution (Dickson et al., 2007). The samples were refrigerated until arriving in the laboratory, where they were preserved at 4°C for analysis. The DIC concentration was analyzed following the coulometric method described by Johnson et al. (1987) with an uncertainty of 3.0 µmol·kg⁻¹ in the Oceanographic Research Institute (IIO-UABC). Certified reference material (CRM AG Dickson, Scripps Institution of Oceanography) was used to ensure accurate readings (≤0.15%). The reference material resulted in an average relative difference of 2.2 ± 1.1 µmol·kg⁻¹, with a maximum of 4 µmol·kg⁻¹ (0.2% error), compared to the certified value. Meanwhile, TA was measured using the open-cell potentiometric titration method at the Marine Environmental Quality Laboratory (LabCAM) of the Institute for Marine and Coastal Research (Bernal et al., 2021) with an uncertainty of 4.0 µmol·kg⁻¹. The carbonate system variables measured *in situ* were compared with meteorological, hydrological, and oceanographic information to understand their influence on these variables. Aragonite (Ω_{arag}) and calcite (Ω_{calc}) saturation levels were calculated with CO2sys v2.3.xls (Lewis and Wallace, 1998), using discrete measurements of SST, salinity, DIC, and TA (Orr et al., 2018). Additionally, the Millero constants were applied because they are suitable for the NBS scale and coastal estuarine environments (Millero, 2010), which are characterized by notable variations in salinity driven by freshwater runoff.

2.2.3 Partial pressure of CO₂ and ocean-atmosphere CO₂ fluxes

The pCO₂ data were measured *in situ* using a Pro-Oceanus CO₂-Pro probe (Bridgewater, Canada) at the surface and bottom in the exposed and protected areas of each bay and compared with those calculated by the couple DIC-TA using CO2sys_v2.3.xls (Lewis and Wallace, 1998). This dataset initially showed similar values; however, by the end of the record (2022), the measured values diverged from the calculated values in both magnitude and trend. As a result, the calculated values were chosen for analysis. These discrepancies may have been caused by sensor drift or calibration errors over time. Additionally, factors, such as debris or water pollution, could have impacted the *in situ* pCO₂ measurements. The wind speed in each area was measured *in situ* on each side of each bay using a GM816 BENETCH digital handheld anemometer (Palo Alto, USA), which also measured air temperature.

The CO₂ flux in the ocean-atmosphere interface (FCO₂) was determined using the following equation:

$$FCO_2 = K_0 \times K_w \times (pCO_2^{sw} - pCO_2^{atm}) \tag{4}$$

where K₀ is the CO₂ solubility coefficient in seawater (mol L⁻¹ atm⁻¹); determined according to (Weiss, 1974) as a function of SST (°K) and SSS; K_w is the gas transfer velocity (cm hour⁻¹), calculated using the equation of Wanninkhof (2014); pCO₂^{sw} is the pCO₂ at the surface (measured in this study); and pCO₂^{atm} is the pCO₂ in the atmosphere, which was obtained from the Ragged Point measuring station (Barbados) of the Earth System Research Laboratories of the NOAA Global Monitoring Network (Lan et al., 2024). This station was the closest to the study area and exhibited similar conditions to those in the Caribbean. A positive FCO₂ value indicates that more CO₂ is present in the ocean than in the atmosphere. Under these conditions, the ocean acts as a CO₂ source. In contrast, negative values indicate that more CO₂ is present in the atmosphere than in the ocean, with the ocean acting as a CO₂ sink.

2.2.4 Underlying drivers of the carbonate system

To determine the main underlying drivers of the pCO₂, pH, and Ω variability in the study area, a first-order Taylor series decomposition method was used for pCO₂, pH, and Ω_{arag}, considering the influence of temperature (T), salinity (S), DIC, and TA. This type of decomposition has been used in other marine carbonate system studies (Lovenduski et al., 2007; Doney et al., 2009b; Gallego et al., 2018; Wright-Fairbanks and Saba, 2022).

The interannual and seasonal surface-water anomalies for any variable X' (ΔpCO₂', ΔpH' and ΔΩ_{arag}') can also be expanded linearly for all variables under consideration:

$$\Delta pCO_2' = \frac{\partial pCO_2}{\partial T} T' + \frac{\partial pCO_2}{\partial S_{FW}} S' + \frac{\partial pCO_2}{\partial DIC} nDIC' + \frac{\partial pCO_2}{\partial TA} nTA' \tag{5}$$

where

$$\frac{\partial pCO_2}{\partial S_{FW}} S' = \frac{\partial pCO_2}{\partial S} S' + \frac{\partial pCO_2}{\partial DIC} DIC'_s + \frac{\partial pCO_2}{\partial TA} TA'_s \tag{6}$$

$$\Delta pH' = \frac{\partial pH}{\partial T} T' + \frac{\partial pH}{\partial S_{FW}} S' + \frac{\partial pH}{\partial DIC} nDIC' + \frac{\partial pH}{\partial ALK} nTA' \tag{7}$$

where

$$\frac{\partial pH}{\partial S_{FW}} S' = \frac{\partial pH}{\partial S} S' + \frac{\partial pH}{\partial DIC} DIC'_s + \frac{\partial pH}{\partial TA} TA'_s \tag{8}$$

$$\Delta \Omega_{arag}' = \frac{\partial \Omega}{\partial T} T' + \frac{\partial \Omega}{\partial S_{FW}} S' + \frac{\partial \Omega}{\partial DIC} nDIC' + \frac{\partial \Omega}{\partial Alk} nTA' \tag{9}$$

where

$$\frac{\partial \Omega_{arag}}{\partial S_{FW}} S' = \frac{\partial \Omega_{arag}}{\partial S} S' + \frac{\partial \Omega_{arag}}{\partial DIC} DIC'_s + \frac{\partial \Omega_{arag}}{\partial TA} TA'_s \tag{10}$$

In addition, freshwater precipitation and evaporation drive correlated variations in surface water DIC' and TA', which have opposite effects on pCO₂. To remove this effect, we use the modified method of Lovenduski et al. (2007), normalizing DIC and TA by salinity (nDIC and nTA, respectively), using (Equation 11), with average salinity represented by Sal_{ref}:

5 <https://www.seabird.com/asset-get.download.jsa?code=250995>

$$nDIC/nTA = \frac{DIC/TA_{spl}}{Sal_{spl}} \times Sal_{ref} \quad (11)$$

The monthly anomaly of the variable after removing the mean monthly climatology (X_0 ; i.e., mean January or mean February), given by $X' = X - X_0$, was used to evaluate change on the interannual time scale. The partial derivative S_{FW} corresponds to the freshwater driver that includes the direct effect of changes in salinity on pCO_2 , pH, and Ω_{arag} and the indirect effect caused by changes in surface DIC and TA (Lovenduski et al., 2007; Doney et al., 2009b; Hauri et al., 2013; Franco et al., 2021). To calculate the partial derivatives, we used the derived routine for CO2SYS-MATLAB (Orr et al., 2018).

Instead of using the deseasonalized series for the seasonal analysis, monthly averages were calculated, and the difference between these and the total average (seasonal amplitude) was used.

Finally, we evaluated differences in conditions between the Gayraca and Chengue Bays and between exposed and sheltered stations with a non-parametric Mann-Whitney test in Minitab v21.1.0. No significant differences were present between the exposed and protected areas of each bay or between the Gayraca and Chengue Bays (see Supplementary Material). Both sites displayed similar patterns; thus, we only describe Gayraca Bay in this study. The results for Chengue Bay can be found in the supplementary material.

3 Results

3.1 Climatic and oceanographic forcing

Contrasting annual patterns in wind and rainfall were observed. The highest wind speeds (until $12 \text{ m}\cdot\text{s}^{-1}$) and minimal rainfall ($\sim 0 \text{ mm}$) were recorded in the first three months of the year related to the intensification of the northeast trade winds between December and March, with seasonal upwelling decreasing temperature (Figure 2A). From September to November, the winds relaxed, and the northward shift in the ITCZ enhanced precipitation, decreased salinity ($\sim 33 \text{ PSU}$; Figure 2B), and increased SST. The intensification in rainfall increased Magdalena River discharge (a proxy for terrestrial runoff; Figure 2C), with the freshwater contribution resulting in biogeochemical changes in the area.

During the study period, a weak La Niña (2017–2018) evolved into a weak El Niño (2018–2019), followed by a moderate La Niña (2020–2022). The upwelling index indicated that upwelling conditions were present throughout much of the year, with weakening in the wet season and strengthening in the dry season (first three months of the year; Figure 3A). Upwelling and rainfall exhibited interannual changes related to ENSO conditions (Figure 3B), with an intensification of upwelling and negative anomalies in rainfall coinciding with the weak El Niño. During

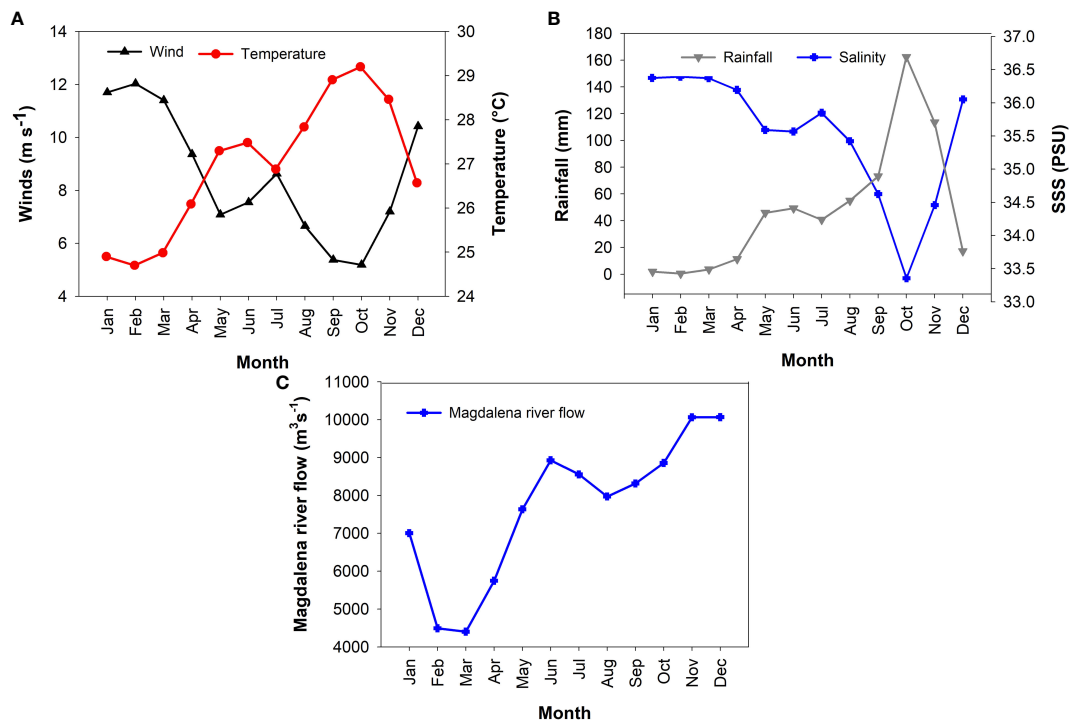


FIGURE 2 Description of the seasonal cycle of wind ($\text{m}\cdot\text{s}^{-1}$) and sea surface temperature (SST, °C) (A), precipitation (mm) and salinity (UPS) (B), and Magdalena River discharge ($\text{m}^3\cdot\text{s}^{-1}$) (C) for a location near the study area ($11^\circ 30' \text{ N}$, $74^\circ 15' \text{ W}$).

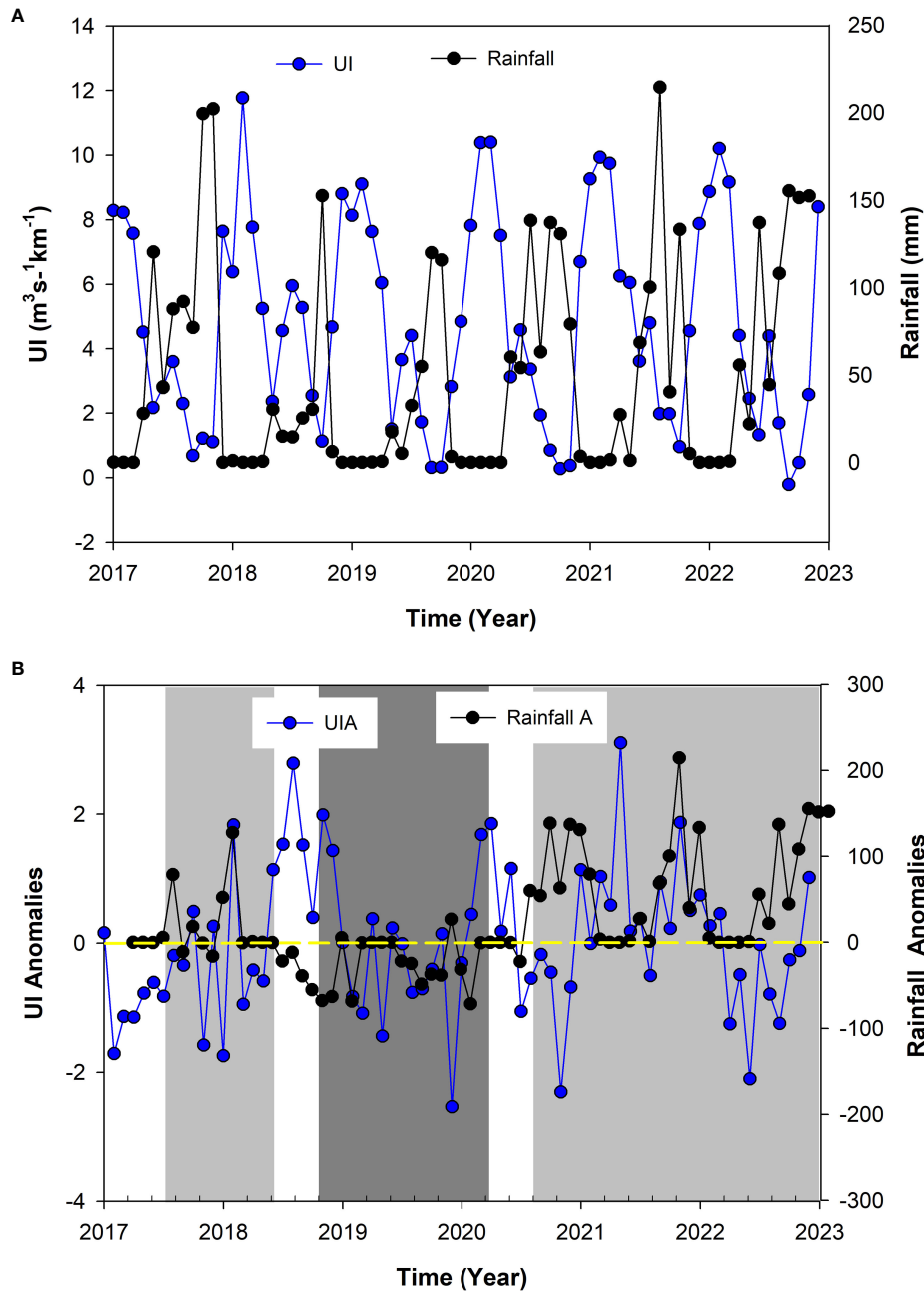


FIGURE 3 Upwelling index (UI) in the Tayrona National Natural Park (TNNP) and accumulated monthly rainfall at the Aeropuerto Simón Bolívar station between March 2017 and October 2022 (A). Deseasonalized anomalies of UI and rainfall over the study period (B). Light gray bars indicate La Niña, and dark gray bars indicate El Niño conditions.

La Niña periods, the strongest negative upwelling anomalies were observed along with positive rainfall anomalies.

In situ data of temperature and salinity revealed significant seasonal variations linked to changes in upwelling intensity and river runoff, associated with the presence of different water masses (Figure 4). During the dry season when upwelling was strongest, the lowest SST values were recorded (24–25°C), and modified Subtropical Underwater (SUWm) predominated, characterized by $SA > 36.6 \text{ g kg}^{-1}$ and $\Theta \sim 22\text{--}23^\circ\text{C}$ (Giraldo, 1994; Hernandez-

Guerra and Joyce, 2000). During the rainy season, warmer waters were present in the study area with features similar to Caribbean Surface Water (CSW, $SA \sim 35.5 \text{ g kg}^{-1}$ and $\Theta \sim 28\text{--}30^\circ\text{C}$; (Hernandez-Guerra and Joyce, 2000). The water column showed minimal vertical variation in temperature, salinity, and dissolved oxygen, indicating uniform mixing (refer to Supplementary Material). However, the T-S mix data from different years revealed variations due to the impact of surface freshwater inputs and/or water masses (Figure 4) (CSW and SUWm).

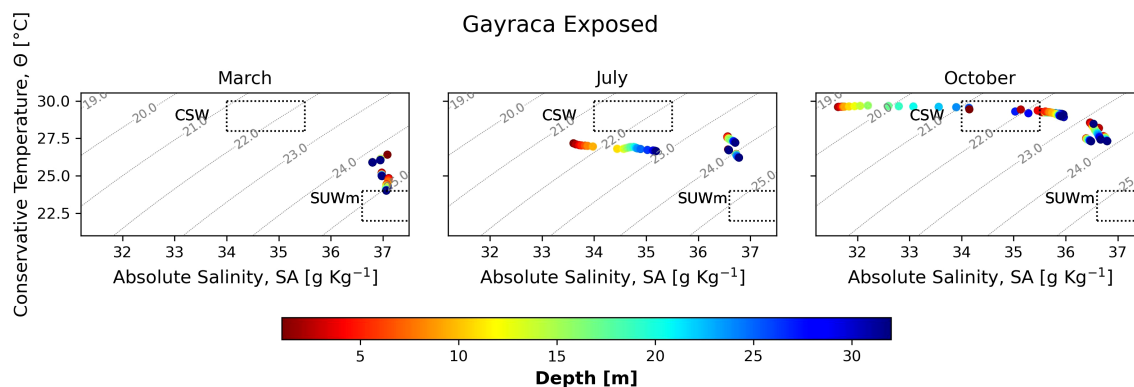


FIGURE 4
Θ-SA diagrams of the exposed area of Gayraca Bay in March, July, and October during 2017 and 2022. The dotted box indicates the conservative temperature and absolute salinity values of the water masses Caribbean Surface Water (CSW) and Subtropical Underwater modified (SUWm).

3.2 Carbon biogeochemistry and saturation state in the Tayrona National Natural Park

No vertical variability was present in the parameters because of the well-mixed water column. Therefore, we only describe surface patterns. The average, maximum, and minimum values are shown in Table 1. The differences in environmental conditions between the dry (enhance upwelling) and wet (increase river runoff) seasons were reflected in the differences in the carbonate system variables. The seasonal carbonate system climatologies showed low SST and pH, but high SSS, DO, DIC, and TA values during the upwelling season (dry conditions) and the opposite in the wet season (Figure 5A). Associated with the low rainfall period of *Veranillo de San Juan*, low SST; pH values below 8.1; high SSS, DIC and TA values; and low DO were observed in June, earlier than expected (July to August).

The time series showed high interannual variability, with SST and SSS consistently exhibiting opposite behavior, marking the changes between dry and wet conditions. During periods of higher SST and lower SSS, lower DO values and higher pH levels were observed, associated with increased terrestrial runoff. As expected, DIC and TA followed a pattern similar to that of SSS, especially in the protected area of Gayraca Bay (Figure 5B).

The water masses observed in the study area exhibited characteristic DIC, TA, pH, and DO signatures, with lower pH

(7.73–8.06) and higher DIC (2082–2122 $\mu\text{mol}\cdot\text{kg}^{-1}$), TA (2316 – 2433 $\mu\text{mol}\cdot\text{kg}^{-1}$), and DO (4.19 – 4.39 $\text{ml}\cdot\text{L}^{-1}$) values associated with SUWm, while higher pH (8.11–8.41) and lower DIC (1799–1990 $\mu\text{mol}\cdot\text{kg}^{-1}$), TA (2032–2172 $\mu\text{mol}\cdot\text{kg}^{-1}$), and DO (3.50 – 4.22 $\text{ml}\cdot\text{L}^{-1}$) values were associated with CSW (Table 2).

During 2018 and 2019, the water samples were classified as neither SUW nor CSW, although the values were close to those of SUW, with low pH and high DIC values. Meanwhile, in July and October 2021, a water mass with characteristics close to those of CSW was observed with high pH, low DIC, and low DO, although the DIC values were higher for October. Finally, in July 2022, no specific water mass could be identified because DIC and pH were low, while TA and DO were high.

The saturation values for Ω_{calc} ranged from 0.34 to 9.98 (average of 4.90), while those for Ω_{arag} ranged from 0.23 to 6.63 (average of 3.35; Figure 6). Both Ω_{calc} and Ω_{arag} exhibited values <1 during February 2022 (0.80 and 0.53, respectively), indicating corrosive conditions for calcium carbonate. These values coincided with waters of low pH (7.99), high DIC (2109 $\mu\text{mol}\cdot\text{kg}^{-1}$), and low TA (2069 $\mu\text{mol}\cdot\text{kg}^{-1}$) associated with the presence of mixing between SUWm and CSW.

The carbonate system variables showed a significant association with ENSO (Figure 7). During the weak La Niña event, anomalies were predominantly positive for pCO_2 and DIC but negative or near zero for TA and Ω_{arag} . In contrast, during the moderate La Niña event, the anomalies alternated, with pCO_2 , DIC and TA showing

TABLE 1 Descriptors of pH, dissolved inorganic carbon (DIC), total alkalinity (TA), sea surface temperature (SST), sea surface salinity (SSS), and dissolved oxygen (DO).

Station	Descriptor	pH	DIC [$\mu\text{mol}\cdot\text{kg}^{-1}$]	TA [$\mu\text{mol}\cdot\text{kg}^{-1}$]	SST	SSS	DO ($\text{ml}\cdot\text{L}^{-1}$)
Gayraca exposed	Average	8.16	2043	2335	27.08	36.03	4.11
	Max.	8.43	2122	2483	29.60	36.94	4.99
	Min.	7.72	1719	2032	24.15	29.63	3.48
Gayraca sheltered	Average	8.14	2044	2350	27.12	35.99	4.10
	Max.	8.46	2147	2602	29.85	36.94	4.85
	Min.	6.86	1770	2052	24.06	29.33	3.58

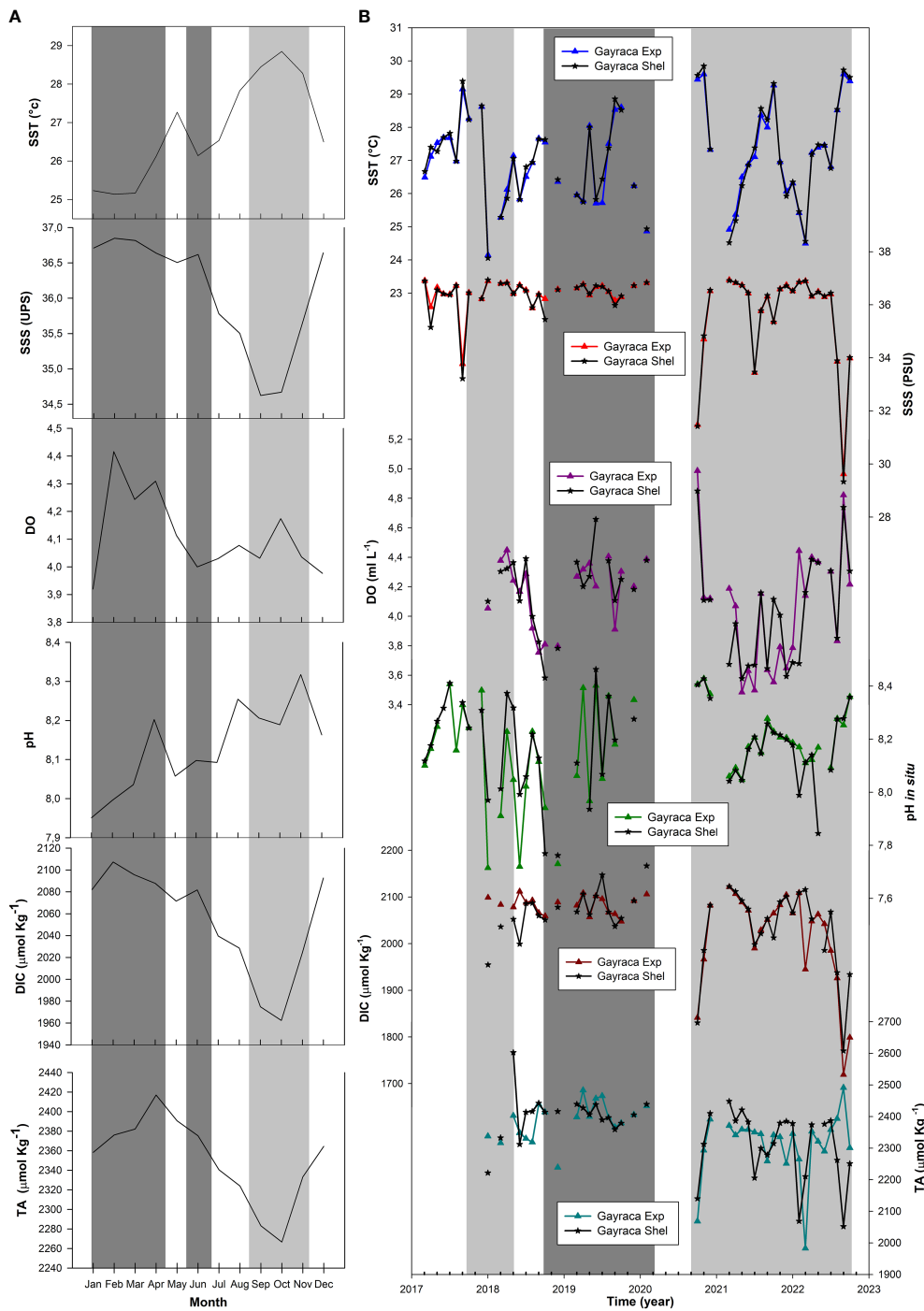


FIGURE 5 Seasonal climatology of sea surface temperature (SST), sea surface salinity (SSS), dissolved oxygen (DO), pH, dissolved inorganic carbon (DIC), and total alkalinity (TA) in Gayraca Bay (A). Dark gray bar indicates the dry season, and light gray bar indicates the wet season. Time series of SST, SSS, DO, pH, DIC, and TA (B). Light gray bars indicate La Niña, and dark gray bars indicate El Niño conditions.

predominantly negative values toward the end of the record, while Ω_{arag} exhibited positive anomalies. Meanwhile, during the weak El Niño event, pCO_2 anomalies were negative, whereas DIC, TA, and Ω_{arag} anomalies were predominantly positive. Conversely, pH anomalies did not exhibit consistent patterns during La Niña or El Niño events.

3.3 Partial pressure of CO₂ and carbon fluxes

Seasonally, the highest pCO_2 values were found in the dry season when upwelling was active, while the lowest were in the season with maximum rainfall and river runoff (Figure 8A). At the interannual

TABLE 2 Values of dissolved inorganic carbon (DIC), total alkalinity (TA) and pH in relation to the water masses recorded for the characteristic months of the climatic seasons in Gayraca Bay.

Time (y-m)	pH	DIC ($\mu\text{mol}\cdot\text{kg}^{-1}$)	TA ($\mu\text{mol}\cdot\text{kg}^{-1}$)	OD ($\text{ml}\cdot\text{L}^{-1}$)	Water Mass
2018_3	7.91	2083.56	2316.20	4.38	Close to SUWm
2018_7	8.02	2087.90	2330.19	4.29	
2018_10	7.94	2059.04	2414.00	3.81	
2019_3	8.06	2081.92	2398.08	4.27	Close to SUWm
2019_7	8.05	2095.69	2465.00	4.30	
2019_10	8.01	2047.56	2378.90	4.30	
2020_3	7.82	2105.76	2433.20	4.39	SUWm
2020_10	8.41	1841.45	2068.30	4.99	CSW
2021_3	8.06	2121.70	2432.50	4.19	SUWm
2021_7	8.21	1989.76	2183.10	3.50	Close to CSW
2021_10	8.23	2065.06	2300.00	3.55	
2022_3	8.11	1945.00	2032.00	4.14	Close to CSW
2022_7	8.09	1985.10	2384.00	4.30	
2022_10	8.36	1799.00	2172.00	4.22	CSW

Lines shaded with dark gray correspond to periods where a specific water mass could not be identified.

scale (Figure 8B), the lowest $p\text{CO}_2$ values, close to atmospheric equilibrium (average of $411 \mu\text{atm}$ for 2019) at the Ragged Point station in Barbados (used as a reference in this study), were recorded during the weak El Niño event and in the second half of 2022, corresponding to the moderate La Niña period. Both periods were characterized by negative upwelling anomalies (Figure 3). The second period showed the lowest recorded values, with an average of $393 \mu\text{atm}$. In contrast, the highest values (mean of $610 \mu\text{atm}$) with higher amplitudes ($\sim 400 \mu\text{atm}$) were observed during the weak La Niña (late 2017-mid 2018) and during the middle of the moderate La Niña (second half of 2021-first half of 2022).

The ocean-atmosphere CO_2 flux values (Figure 9) analyzed between March 2017 and October 2022 were mostly positive. Thus, the area acted as a source of CO_2 . The CO_2 fluxes were higher in the

exposed zone (mean $35.4 \text{ mmol}\cdot\text{m}^{-2}\cdot\text{day}^{-1}$) than in the protected (mean $16.8 \text{ mmol}\cdot\text{m}^{-2}\cdot\text{day}^{-1}$) zone. Negative flux values (sink behavior) were very small (close to zero) and were observed mainly during the same periods of negative upwelling anomalies explained above (Figure 3) (i.e., during the weak El Niño and the second half of 2022 [the moderate La Niña period]).

3.4 Trends of carbonate system variables in the Northeastern Colombian Caribbean Coast

Despite the increasing trend in the CO_2 concentration at the Ragged Point (Bermuda) station (Figure 10A), the carbonate system

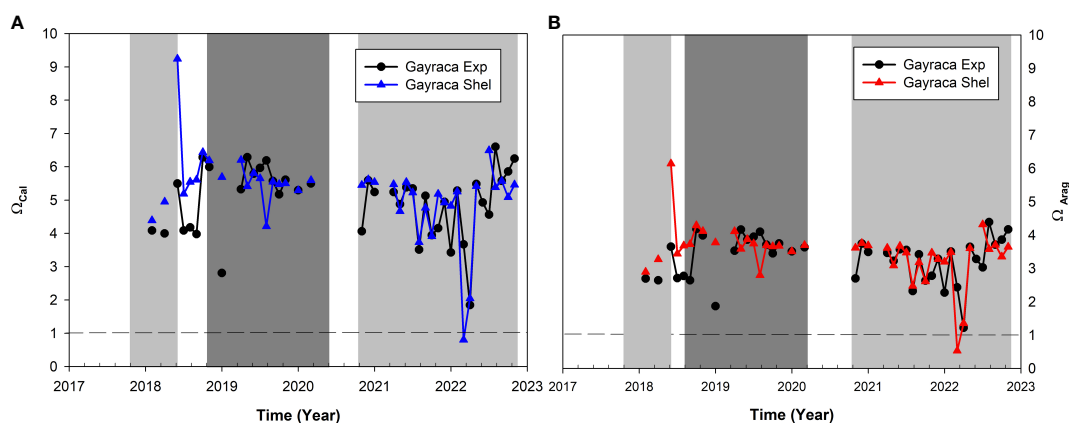
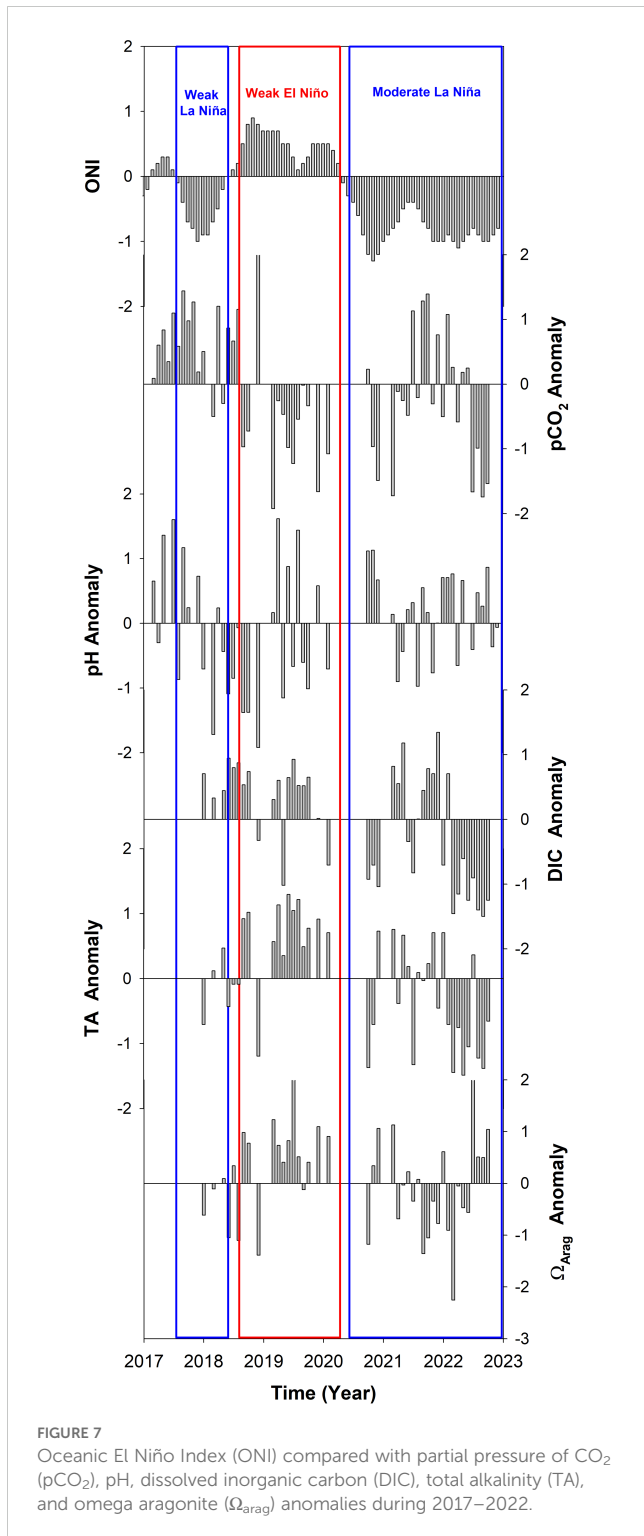


FIGURE 6 Calcium carbonate saturation state in Gayraca Bay: calcite (Ω_{calc}) (A) and aragonite (Ω_{arag}) (B). Light gray bars indicate La Niña, and dark gray bars indicate El Niño conditions.



variables showed mainly a decreasing trend over the study period (2017–2022) (Figure 10): pCO₂ ($-0.5464 \mu\text{atm}\cdot\text{y}^{-1}$), nDIC ($-0.6828 \mu\text{mol}\cdot\text{kg}^{-1}\cdot\text{y}^{-1}$), DIC ($-2.8685 \mu\text{mol}\cdot\text{kg}^{-1}\cdot\text{y}^{-1}$), and TA ($-2.74 \mu\text{mol}\cdot\text{kg}^{-1}\cdot\text{y}^{-1}$) (Figures 10B, E, F and G, respectively). Only pH

(Figure 10C) (0.0015) showed a slight increasing trend, while Ω_{arag} (-0.0008) and nTA ($-0.0768 \mu\text{mol}\cdot\text{kg}^{-1}\cdot\text{y}^{-1}$) (Figures 10D, H) showed minimal decreasing trends.

3.5 Underlying drivers of the carbonate system

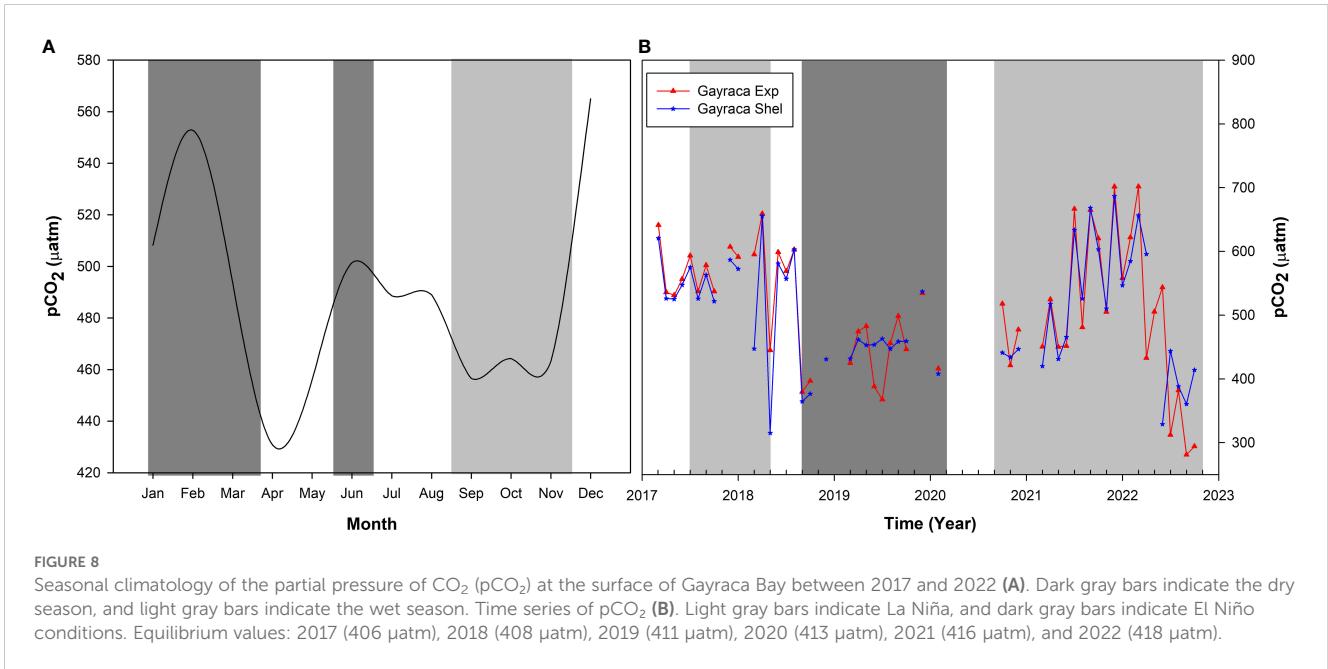
At the seasonal scale, we observed that TA was an important driver of changes in pCO₂ (Figure 11A). This was observed mainly in the dry season (December to April), although during February and July, which are months with high upwelling activity, DIC increased its positive effect on pCO₂. In the wet season, the effect was negative, which coincided with the relationship between DIC-TA and SSS (see Supplementary Material). Also, SST exhibited an important contribution: it was the second most important driver in the dry season and the main driver at the end of the wet season (October to November).

TA was an important driver of pH changes (Figure 11B), although DIC and freshwater, includes the direct effect of salinity changes due to freshwater input (S_{FW}) also exhibited important contributions. DIC was the main driver in February, with its effect increasing from May to July. Freshwater was the main driver of change (positive effect) in pH during the wet season and in August. Finally, the main driver of changes in Ω_{arag} was TA (Figure 11C), with important negative contributions to DIC in February, June, and July (dry season) and a positive contribution in March.

At the interannual scale, TA was the main driver of pCO₂, pH, and Ω_{arag} changes (Figures 11D, E, F), with some periods where DIC was the dominant driver. For pCO₂, these two drivers had positive effects at the beginning of the record and between mid-2021 and 2022. The contribution of S_{FW} to CO₂ increased at the end of the record, between the end of 2020 and the end of 2022, which coincided with a moderate La Niña event. TA had a negative influence on pH at the beginning of the record but a positive influence between the end of 2020 and the middle of 2022. Finally, the contribution of TA to pCO₂ was mainly negative at the beginning of the record, as well as between the end of 2020 and mid-2022.

4 Discussion

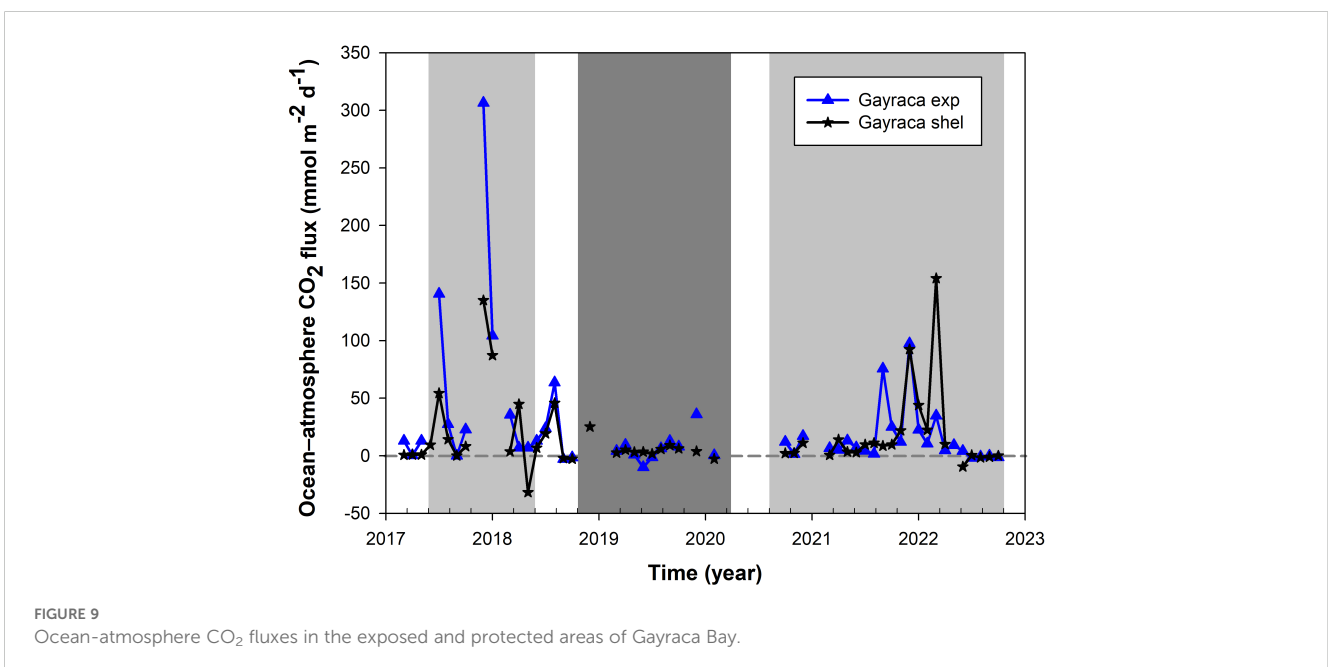
We analyzed the temporal variation of the TNNP carbonate system from 2017 to 2022. Upwelling and fluvial runoff influenced seasonal patterns, while interannual variability was modulated by ENSO events. These factors alternated between marine and estuarine conditions, shaping the chemistry of the carbonate system in the study area. The results highlight the high variability of oceanographic processes in coastal regions, emphasizing the need for a holistic understanding of the system that considers chemical, physical, and biological variables, as well as ocean-atmosphere interactions to identify the underlying mechanisms.



4.1 Seasonal variability of oceanographic and biogeochemical conditions

The TNNP is a principal site for seasonal La Guajira upwelling (Rueda-Roa and Muller-Karger, 2013). Alongshore winds during the dry season (December to April) and *Veranillo de San Juan* (July) result in an upwelling of a subsurface water mass (Sarmiento-Devia et al., 2013; Herrera-Fajardo et al., 2017; Correa-Ramirez et al., 2020), characterized by a low temperature and high salinity water mass identified as modified Subtropical Underwater (Correa-Ramirez et al., 2020). This water mass was associated with lower pH values (average 8.0), high DIC, and high TA that resulted in natural acidification conditions similar to those observed in other

tropical upwelling regions, such as the Gulf of Papagayo (Sánchez-Noguera et al., 2018) and Gulf of Tehuantepec (Chapa-Balcorta et al., 2015). During the rainy season, when more river runoff was observed from the Magdalena River and other nearby rivers (September to November), pH values were higher (~8.2) than in the dry season, reflecting mixing in the coastal zone (Carstensen and Duarte, 2019). In this period, DIC and TA values were lower due to freshwater dilution (Salisbury et al., 2009), which was associated with increased river runoff due to more rainfall, contributing to the formation of Caribbean surface water. Cervantes-Diaz et al. (2022) reported similar results for the Gulf of Mexico, observing low DIC values associated with this water mass. The highest pH values (average pH of ~8.25) were recorded



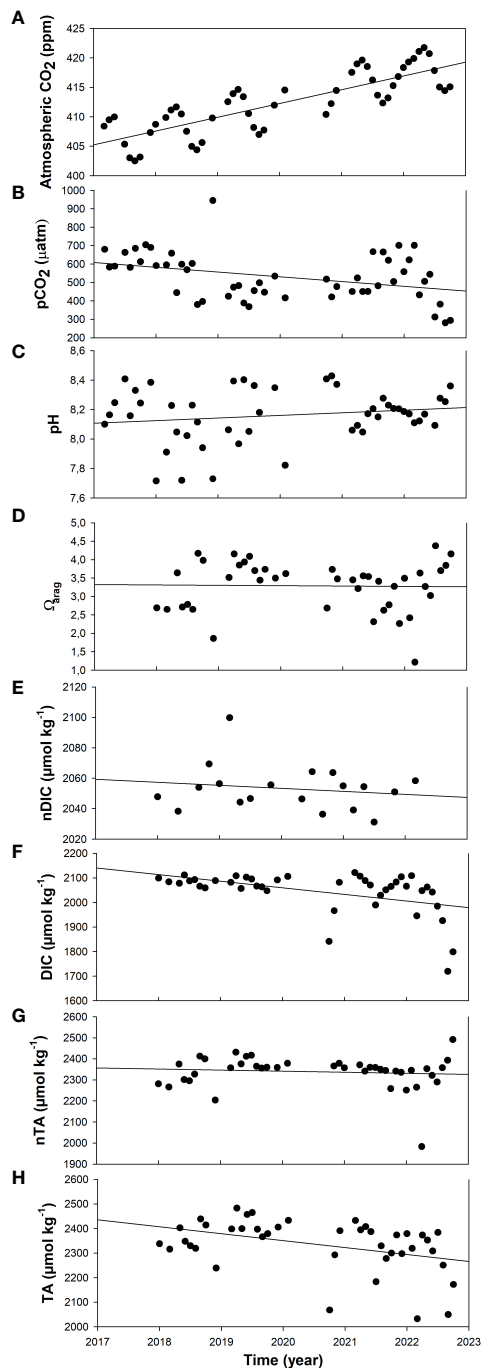


FIGURE 10

Trends in atmospheric CO_2 records from the Ragged Point measuring station (Barbados) (A), and the carbonate system variables, partial pressure of CO_2 (pCO_2) (B), pH (C), calcium carbonate saturation state of aragonite (Ω_{arag}) (D), salinity-normalized dissolved inorganic carbon (nDIC) (E), dissolved inorganic carbon (DIC) (F), salinity-normalized total alkalinity (nTA) (G), and total alkalinity (TA) (H) in the exposed and protected areas of Gayraca Bay.

during transition periods (April and August), probably because upwelling relaxed and freshwater inputs were low. The results of this study also align with descriptions of other areas influenced by fluvial inputs that modulate ocean chemistry, particularly DIC and TA (Lefèvre et al., 2014, 2021).

The waters in the Gayraca and Chengue sites did not show the typical salinity and temperature values for CSW and SUW, probably due to changes due to evaporation and the influence of continental runoff (Guerrero and Piola, 1997; Tomczak, 1999; Cervantes-Díaz et al., 2022). Similarly, diffusion, lateral mixing, currents, and their fluctuations have been shown to modify salt and heat balances and alter water mass characteristics (Guerrero and Piola, 1997).

The seasonal behavior of pCO_2 showed the highest values during the dry season (December–March and June) coinciding with the season of highest wind speeds, upwelling conditions, lower SST, and higher DIC/TA. Hernández-Ayón et al. (2013) explained that upwelled water contains high concentrations of DIC, leading to higher seawater pCO_2 than atmospheric pCO_2 , favoring a positive ocean-to-atmosphere.

4.2 Interannual variability related to ENSO events

The interannual variability patterns of the oceans are primarily modulated by the main atmospheric and ocean-atmosphere climate modes (Wang and Schimel, 2003). In the tropical Pacific, ENSO is the most important force in marine physics and biogeochemistry (Doney et al., 2009b). Also, the northeastern Colombian Caribbean coast exhibited interannual variability related to contrasting climatic conditions associated with ENSO events. River runoff, including water from the Ciénaga Grande de Santa Marta and Magdalena River, notably affects the oceanographic conditions of the TNNP, which has been generally only associated with upwelling. Nonetheless, river runoff inputs were a crucial determinant of the conditions in the area during the study period, which was evident due to the high rainfall recorded from 2017 to 2018 and from the end of 2020 to 2022 during La Niña events. An increase in river runoff during La Niña has been observed in several coastal areas adjacent to large rivers like the Magdalena River (Restrepo and Kjerfve, 2000; Restrepo et al., 2006), such as those adjacent to the Amazon and Congo Rivers (Lefèvre et al., 2014, 2021; Ibáñez et al., 2015), with consequences for the biogeochemistry of the nearby ocean (Bates and Hansell, 2004).

During El Niño, a decrease in rainfall and negative upwelling anomalies led to lower pCO_2 and a lower ocean-atmosphere CO_2 flux, which agrees with the observations of Feely et al. (1999, 2002) and Doney et al. (2009b) for the Pacific Ocean during El Niño events. These authors documented a strong correlation between the reduction of the CO_2 flux into the atmosphere and the onset of El Niño. During this period, discrepancies between DIC/TA (high) and pCO_2 (low) were observed, which arose primarily due to reduced upwelling, which limits the influx of CO_2 into surface waters (Feely et al., 1999). This results in lower pCO_2 levels, even when DIC and TA remain relatively high. Similarly, diminished CO_2 -rich terrestrial runoff can contribute to this effect (Salisbury et al., 2009). Total alkalinity and DIC generally increases during El Niño due to changes in water mass properties due increase evaporation (Feely et al., 1999; Zeebe and Wolf-Gladrow, 2001). Elevated TA enhances the buffering capacity of a system, moderating pH changes and altering carbonate chemistry speciation (Sabine and Feely, 2007). This buffering can

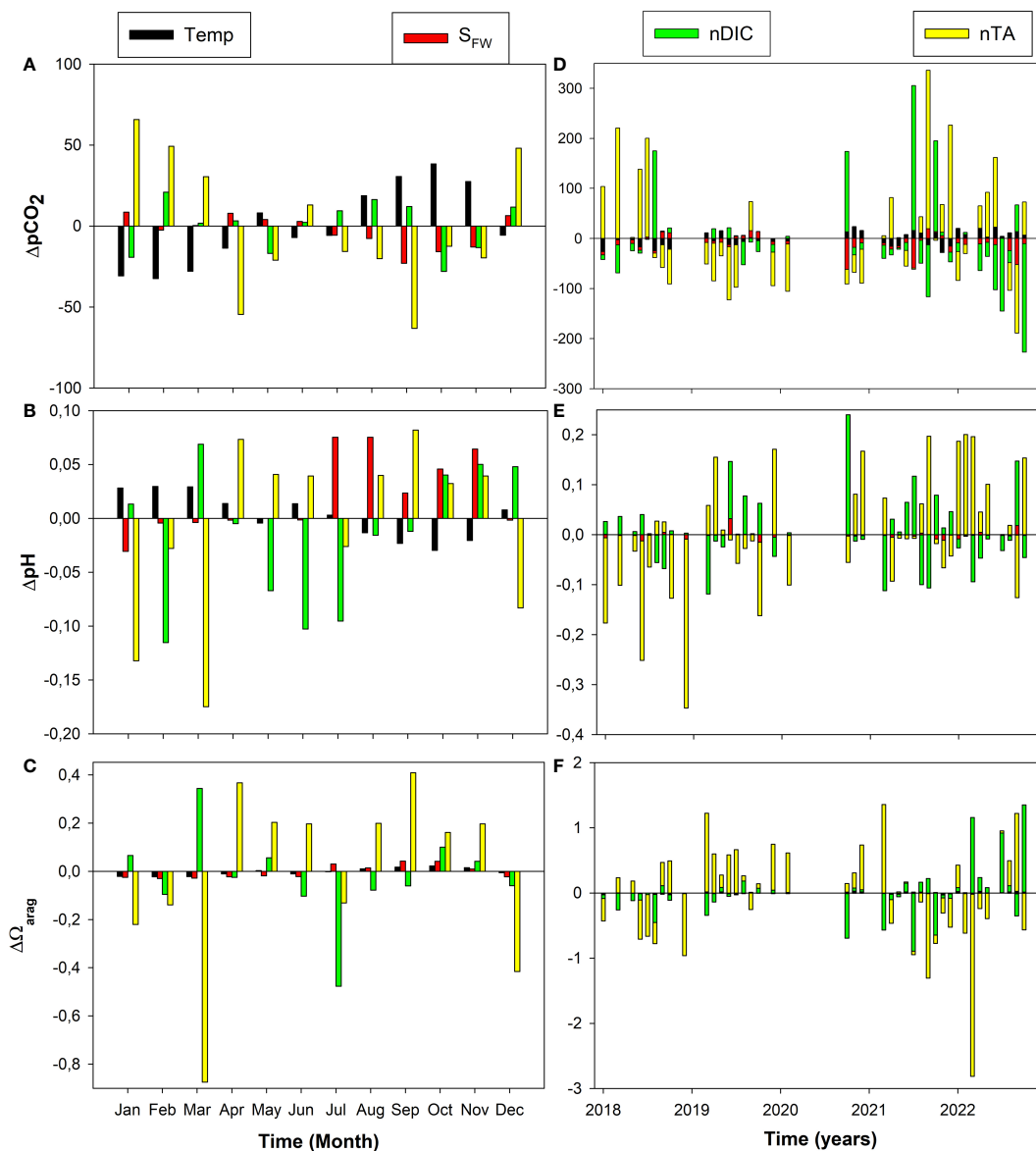


FIGURE 11
 Factors driving seasonal variability in carbonate system variables, partial pressure of CO₂ (pCO₂) (A), pH (B), and calcium carbonate saturation state of aragonite (Ω_{arag}) (C) in Gayraca Bay, corresponding to components of a Taylor series decomposition. Drivers of interannual variability in carbonate system variables: pCO₂ (D), pH (E), and Ω_{arag} (F). The contributions of sea surface temperature (black), freshwater (red), dissolved inorganic carbon (DIC, green), and total alkalinity (TA, yellow) are shown.

reduce the fraction of DIC existing as CO₂(aq) or pCO₂, even with higher overall carbon content. Additional influences include biological activity and temperature effects on CO₂ solubility (Takahashi et al., 2009).

During La Niña events, greater variability in conditions was observed related to increased river runoff and changes in upwelling patterns. During the weak La Niña and in the middle of the moderate La Niña, positive pCO₂, TA, and DIC anomalies coincided with positive upwelling anomalies and an increase in the CO₂ flux, which is consistent with the increase in the CO₂ flux observed at the onset of La Niña in the Pacific Ocean (Feely et al., 1999, 2002; Doney et al., 2009b). However, at the beginning and end of the moderate La Niña event, the behavior was opposite to what was previously described, with negative anomalies in pCO₂, TA, and DIC observed,

accompanied by a decrease in CO₂ flux. Additionally, during certain periods, a decoupling between DIC-TA and pCO₂ was evident. While DIC and TA were low due to freshwater dilution (Salisbury et al., 2009), pCO₂ remained high, possibly influenced by factors such as inputs from CO₂-rich rivers and upwelling, increased respiration, and reduced buffering capacity (Bates and Hansell, 2004; Sabine and Feely, 2007; Salisbury et al., 2009).

During the middle of the moderate La Niña event (July 2021), a water mass arrived at the surface with characteristics similar to those of SUWm but with low DIC. This suggests that the biogeochemical characteristics of the water reaching the surface during the upwelling season were influenced by continental inputs, which agrees with what was reported by Correa-Ramirez et al. (2020). In this study, the pH anomalies were found to be more

irregular and less systematic compared to those of $p\text{CO}_2$, total alkalinity (TA), and dissolved inorganic carbon (DIC). This discrepancy stems from the complex interplay of factors influencing ocean pH. Unlike $p\text{CO}_2$, TA, and DIC, which generally align with large-scale, systematic processes (Takahashi et al., 2009a), pH is highly sensitive to localized, non-linear, and transient factors that can obscure clear patterns (Hofmann et al., 2011). Additionally, biological processes, such as photosynthesis, respiration, and calcification, drive rapid and localized changes in pH (Duarte et al., 2013). These processes often lack consistency due to their reliance on variables like light availability, organism distribution, and the time of day (Waldbusser and Salisbury, 2014; Waldbusser et al., 2016). In addition, the logarithmic nature of the pH scale further amplifies the effects of even small changes in $[\text{H}^+]$, resulting in notable pH shifts (Zeebe and Wolf-Gladrow, 2001). This property makes pH anomalies more pronounced and erratic compared to those of TA, DIC, or $p\text{CO}_2$.

4.3 Carbonate saturation state, anomalous events, and their implications

A notable variation was observed in the saturation states of aragonite and calcite due to the contrasting seasonal and interannual conditions of the region. Despite this variability, saturation states generally remained within optimal ranges for calcification. This contrasts with findings by Norzagaray-López et al. (2017) for coral reefs in Cabo Pulmo, Mexico, where low variability in saturation states was reported. These differences highlight that the northeastern Colombian Caribbean region experiences extreme conditions, necessitating a high level of adaptation by local coral communities.

On a seasonal scale, lower saturation states were recorded during the dry season, coinciding with natural acidification linked to the influx of upwelling waters, as previously noted. In contrast, higher saturation states occurred during the minor and major rainy seasons. At the interannual scale, saturation state anomalies for Ω_{arag} were predominantly negative during La Niña events and positive during El Niño events. This interannual variability reflects shifts in nutrient availability, light intensity, and temperature, which are critical drivers of productivity in the reef zone of the TNNP. Despite these fluctuations, benthic primary productivity in the TNNP has been found to remain relatively stable (Eidens et al., 2014), which may contribute to the resilience of these coral communities to anthropogenic disturbances and climate change. However, changes in the environmental conditions of the region could result in high stress for reef formations.

During the moderate La Niña event in early 2022, undersaturated levels (<1) of Ω_{calc} and Ω_{arag} were observed. These were linked to the mixing Subtropical Underwater (SUW, low pH) and Coastal Surface Water (CSW, low DIC). Such conditions could challenge coral calcification in the area, particularly under future climate change scenarios. Extreme events in the Caribbean Sea, including cold fronts from the north (Montoya-Sánchez et al., 2018) and tropical storms, are also expected to intensify. Although there is no consensus on the effects of climate change in upwelling areas, several studies suggest

potential changes in their intensity, timing, and spatial structure (Bakun, 1990; Bakun et al., 2015; Wang et al., 2015).

In the TNNP, increased upwelling intensity could result in higher concentrations of DIC and elevated CO_2 fluxes to the atmosphere during stronger winds, further reducing saturation states. Similarly, changes in hydrological cycles, including increased rainfall associated with global warming (Trenberth, 1998; Allan et al., 2020; Liu et al., 2020), may enhance mixing between SUW and coastal inputs low in DIC. This could create more corrosive water, posing risks to the survival of existing coral formations in the area.

4.4 CO_2 fluxes from the northeastern Colombian Caribbean coast

During the study period, the calculated CO_2 fluxes were predominantly positive, indicating that the area primarily acted as a CO_2 source. The highest flux values were recorded when local wind speeds peaked, particularly during the *Veranillo de San Juan* (July to August), when water temperatures were also elevated. Furthermore, positive upwelling anomalies were linked to increased ocean-atmosphere CO_2 fluxes. The relationship between wind speed and ocean-atmosphere gas exchange has been extensively reviewed by Wanninkhof (1992, 2014).

Using interpolated monthly mean surface ocean $p\text{CO}_2$ and atmospheric $p\text{CO}_2$ data for the Caribbean, Takahashi et al. (2014) reported that positive pressure differences between the ocean and atmosphere persisted throughout most of the year. Exceptions were observed from January to March, when values were slightly negative ($>-30 \mu\text{atm}$), although annual net fluxes remained positive.

4.5 Underlying drivers of the carbonate system

Understanding the factors that drive changes in carbonate system variables is crucial for predicting their responses to both natural variability and climate change effects. In the surface waters of the study area, the behavior of $p\text{CO}_2$, pH, and Ω_{arag} was primarily influenced by seasonal and interannual variations in TA and DIC. This was attributed to freshwater inputs and their effects on the physical and chemical conditions of coastal areas near riverine runoff. The relationship between these drivers, TA and DIC, and their impact on CO_2 exhibited shifts in coupling, influenced by the dominance of specific processes depending on the prevailing biogeochemical and physical dynamics of the system, such as biological activity and mixing processes.

At the seasonal and interannual scales, $p\text{CO}_2$ variability was primarily driven by changes in DIC and TA. This is attributed to the fact that, under estuarine conditions, the buffer sensitivity factors by DIC and TA-induced are generally of similar magnitude. As a result, changes in DIC and TA during gas exchange and biogeochemical processes play a crucial role (Zeebe and Wolf-Gladrow, 2001; Waldbusser et al., 2016; Cai et al., 2021). In addition, the sensitivity of an estuarine water mass can differ

depending on the TA value of the river endmember. Under conditions of low-salinity, estuaries that receive inputs from low-TA rivers show greater sensitivity to the addition of CO₂ than estuaries that receive inputs from high-TA rivers; this has important implications for pCO₂, pH, and Ω_{arag} (Cai et al., 2021).

In this study, during months with increased upwelling activity, which resulted in colder subsurface water with higher DIC content at the surface, a slight damping of this factor on TA on pCO₂ was observed. Furthermore, during La Niña, increased rainfall enhanced freshwater influx, resulting in dilution that notably impacted both DIC and TA.

The sensitivity of pH, pCO₂, and Ω_{arag} in an estuarine water body can vary greatly depending on the TA value of the river endmember. This is because the DIC: TA ratio of the river (~1.0) changes much more rapidly in estuaries that receive inputs from low-TA rivers than in those that receive inputs from high-TA rivers (Cai et al., 2021). Additionally, it has been found that long rivers in tropical areas, such as the Amazon River (Cai et al., 2021) and the Orinoco River, have low TA (Cai et al., 2021). In this study, we also detected a lower TA signal from the Magdalena River, which increased the sensitivity of the carbonate system variables. Furthermore, much of the seasonality of TA is driven by changes in seasonal SSS due to rainfall or ice melting (Gregor and Gruber, 2021).

The variability in pH was mainly modulated by TA followed by DIC and S_{FW}. During the first part of the year, water with higher TA/DIC and lower SST entered the study area, negatively affecting pH. Additionally, higher SSS were recorded due to lower precipitation, less river runoff, and the contribution of upwelled water. Conversely, during the rainy season, the arrival of river runoff with low TA, DIC, and higher SST, along with dilution effects, resulted in an increase in pH. Increased nutrient inputs from rivers can lead to a high biological removal of CO₂ and, consequently, alkalization and an increased buffering capacity in surface waters (Borges and Gypens, 2010). Given that the seasonal cycle of TA in the study area exhibited a greater amplitude than that of SST, the change in pH was not primarily driven by the latter, as has been observed in other coastal areas (Doney et al., 2009b). During upwelling periods (Feb-Mar), DIC compensated TA. However, since the inputs were not as high and the upwelled water in the study area had lower DIC (younger) than that of the Pacific Ocean, they did not outweigh the effects of other variables.

Similarly, the variability of Ω_{arag} at the seasonal scale was mainly modulated by TA, followed by DIC, the latter being the main driver of change during months of coastal upwelling, which provided subsurface water with low pH and low Ω_{arag} content. The effect of DIC on pCO₂, pH, and Ω_{arag} has been widely documented for upwelling zones (Feely et al., 2008; Turi et al., 2016; Addey et al., 2021). In the latter part of the year, TA positively affected Ω_{arag} due to weakened upwelling. At the interannual scale, the main driver of Ω_{arag} change was also TA, confirming that alternating low and high river runoff conditions, due to changes in rainfall, modulated the system at this temporal scale. Lower Ω values occur naturally around most river mouths because they gather runoff from watershed soils, which typically contain carbonic acid, a by-product of organic decomposition (Salisbury et al., 2009). In addition, high rainfall can result in low SSS, and due to notable

freshwater inputs, Ω_{arag} can also be suppressed by the reduction of [Ca²⁺] and [CO₃²⁻] in low-salinity areas, as Ω depends on their concentrations (Salisbury et al., 2008; Feely et al., 2018).

Finally, the observed trends in pH and pCO₂ were primarily driven by a decrease in DIC and TA, attributed to an increased input of river runoff, despite rising atmospheric CO₂ levels. This behavior stands in contrast to the typical ocean acidification trends observed in other regions.

4.6 The importance of the time series of the northeastern Colombian Caribbean coast and future actions

For the first time, a time series of the carbonate system variables is presented for the TNNP, along with a biogeochemical characterization of the shallow water masses of CSW and SUW. River runoff and Southern Caribbean upwelling influence this area on the northeastern coast of the Colombian Caribbean. The observed seasonal and interannual behavior revealed the complexity of oceanographic conditions in coastal regions where oceanic and continental influences alternate, especially in areas with notable fluvial freshwater inputs. In addition, patterns of variability in carbonate system variables were evident from year to year.

This study is important for understanding future ocean acidification scenarios in the context of climate change because characterizing the natural variability of a system is the first step in comprehending anthropogenic influences. A holistic understanding of the system (considering nutrient levels, biological activity, the redox state, and water mixing) is essential for identifying the underlying mechanisms. Therefore, it is necessary to continue monitoring the carbonate system of the TNNP to define an accurate baseline for the seasonal climatological cycle. Additionally, we recommend installing equipment to continuously monitor the TNNP to quantify high-frequency (e.g., daily and monthly) changes. Biological variables, such as those associated with respiration and photosynthesis, may influence the carbonate system; however, in this study, we cannot speculate how they may affect the carbonate system of the TNNP because we did not analyze biological data.

Data availability statement

The raw data supporting the conclusions of this article will be made available by the authors, without undue reservation.

Author contributions

CR-V: Conceptualization, Data curation, Formal analysis, Funding acquisition, Investigation, Methodology, Project administration, Resources, Software, Supervision, Validation, Visualization, Writing – original draft, Writing – review & editing. MM-R: Data curation, Investigation, Methodology, Software, Visualization, Writing – review & editing. JH-A:

Conceptualization, Data curation, Funding acquisition, Investigation, Methodology, Supervision, Writing – review & editing.

Funding

The author(s) declare financial support was received for their research, authorship, and/or publication of this article. This research was funded with resources from the National Investment Projects Bank (BPIN), project “*Investigación científica hacia la generación de información y conocimiento de las zonas marinas y costeras de interés de la nación* [Scientific research aimed at generating information and knowledge of the marine and coastal areas of national interest]”, project code 202300000000039 of the José Benito Vives de Andrés Institute for Marine and Coastal Research (INVEMAR) of Colombia.

Acknowledgments

We thank the researchers of the Oceanography and Climate Line and the Marine Instrumentation Laboratory of the Marine and Coastal Geosciences program of INVEMAR, who contributed to collecting samples and data in the field. Special thanks to researcher María Camila Bernal for her field support, as well as to Sebastián Contreras Fernández, Wilberto Pacheco Paternina, and Lorenzo Portillo Cogollo for their assistance with figures. Additionally, we would like to express our gratitude to the researchers and technicians of the CO₂ System Laboratory of the Oceanographic

Research Institute (IIO) of Universidad Autónoma de Baja California for their assistance in laboratory analysis. We would also like to express our thanks to Researcher Ana Franco for her support in the Taylor Series Decomposition analysis. Finally, we want to express our gratitude to the reviewers, especially reviewer 1 who provided constructive feedback to improve this article.

Conflict of interest

The authors declare that the research was conducted in the absence of any commercial or financial relationships that could be construed as a potential conflict of interest.

Publisher's note

All claims expressed in this article are solely those of the authors and do not necessarily represent those of their affiliated organizations, or those of the publisher, the editors and the reviewers. Any product that may be evaluated in this article, or claim that may be made by its manufacturer, is not guaranteed or endorsed by the publisher.

Supplementary material

The Supplementary Material for this article can be found online at: <https://www.frontiersin.org/articles/10.3389/fmars.2024.1305542/full#supplementary-material>

References

- Addey, C. I., Jiang, Z.-P., Chen, J., Afelumo, A. J., Adesina, B. R., and Osanyintuyi, A. J. (2021). The variability of partial pressure of carbon dioxide (pCO₂) in a river-influenced coastal upwelling system: A case of the northeast Pacific coast. *J. Geosci. Environ. Prot.* 9, 133–148. doi: 10.4236/gep.2021.97009
- Allan, R. P., Barlow, M., Byrne, M. P., Cherchi, A., Douville, H., Fowler, H. J., et al. (2020). Advances in understanding large-scale responses of the water cycle to climate change. *Ann. N Y Acad. Sci.* 1472, 49–75. doi: 10.1111/nyas.1472.1
- Astor, Y. M., Lorenzoni, L., Thunell, R., Varela, R., Muller-Karger, F., Troccoli, L., et al. (2013). Interannual variability in sea surface temperature and fCO₂ changes in the Cariaco Basin. *Deep Sea Res. Part II: Topical Stud. Oceanography* 93, 33–43. doi: 10.1016/j.dsr2.2013.01.002
- Astor, Y. M., Scranton, M. I., Muller-Karger, F., Bohrer, R., and Garcia, J. (2005). fCO₂ variability at the CARIACO tropical coastal upwelling time series station. *Mar. Chem.* 97, 245–261. doi: 10.1016/j.marchem.2005.04.001
- Bakun, A. (1973). *Coastal upwelling indices, west coast of North America*. 1946–1971.
- Bakun, A. (1990). Global climate change and intensification of coastal ocean upwelling. *Sci.* (1979) 247, 198–201. doi: 10.1126/science.247.4939.198
- Bakun, A., Black, B. A., Bograd, S. J., García-Reyes, M., Miller, A. J., Rykaczewski, R. R., et al. (2015). Anticipated effects of climate change on coastal upwelling ecosystems. *Curr. Clim Change Rep.* 1, 85–93. doi: 10.1007/s40641-015-0008-4
- Bates, N. R., and Hansell, D. A. (2004). Temporal variability of excess nitrate in the subtropical mode water of the North Atlantic Ocean. *Mar. Chem.* 84, 225–241. doi: 10.1016/j.marchem.2003.08.003
- Bayraktarov, E., Pizarro, V., and Wild, C. (2014). Spatial and temporal variability of water quality in the coral reefs of Tayrona National Natural Park, Colombian Caribbean. *Environ. Monit. Assess.* 186, 3641–3659. doi: 10.1007/s10661-014-3647-3
- Bayraktarov, E., and Wild, C. (2014). Spatiotemporal variability of sedimentary organic matter supply and recycling processes in coral reefs of Tayrona National Natural Park, Colombian Caribbean. *Biogeosciences* 11, 2977–2990. doi: 10.5194/bg-11-2977-2014
- Bernal, C., Gómez Batista, M., Sanchez-Cabeza, J. A., Cartas-Aguila, H., Herrera-Merlo, J., Ruiz-Rodríguez, G., et al. (2021). “Determinación de alcalinidad total en agua de mar utilizando dispensador manual,” in *Método de titulación en celda abierta* (Santa Marta).
- Borges, A. V., and Gypens, N. (2010). Carbonate chemistry in the coastal zone responds more strongly to eutrophication than ocean acidification. *Limnol Oceanogr* 55, 346–353. doi: 10.4319/lo.2010.55.1.0346
- Cai, W.-J., Feely, R. A., Testa, J. M., Li, M., Evans, W., Alin, S. R., et al. (2021). Natural and anthropogenic drivers of acidification in large estuaries. *Ann. Rev. Mar. Sci.* 13, 23–55. doi: 10.1146/annurev-marine-010419-011004
- Carstensen, J., and Duarte, C. M. (2019). Drivers of pH variability in coastal ecosystems. *Environ. Sci. Technol.* 53, 4020–4029. doi: 10.1021/acs.est.8b03655
- Cervantes-Díaz, G. Y., Hernández-Ayón, J. M., Zirino, A., Herzka, S. Z., Camacho-Ibar, V., Norzagaray, O., et al. (2022). Understanding upper water mass dynamics in the Gulf of Mexico by linking physical and biogeochemical features. *J. Mar. Syst.* 225, 103647. doi: 10.1016/j.jmarsys.2021.103647
- Chapa-Balcorta, C., Hernandez-Ayon, J. M., Durazo, R., Beier, E., Alin, S. R., and López-Pérez, A. (2015). Influence of post-Tehuano oceanographic processes in the dynamics of the CO₂ system in the Gulf of Tehuantepec, Mexico. *J. Geophys. Res. Oceans* 120, 7752–7770. doi: 10.1002/2015JC011249
- Correa-Ramirez, M., Rodriguez-Santana, A., Ricaurte-Villota, C., and Paramo, J. (2020). The Southern Caribbean upwelling system off Colombia: Water masses and mixing processes. *Deep Sea Res. I Oceanogr Res. Pap* 155, 103145. doi: 10.1016/j.dsr.2019.103145
- Da, F., Friedrichs, M. A. M., St-Laurent, P., Shadwick, E. H., Najjar, R. G., and Hinson, K. E. (2021). Mechanisms driving decadal changes in the carbonate system of a coastal plain estuary. *J. Geophys. Res.: Oceans* 126, e2021JC017239. doi: 10.1029/2021JC017239

- Díaz, J., Barrios, L., Cendales, M., Garzón-Ferreira, J., Geister, J., López-Victoria, M., et al. (2000). [amp]Acuereas coralinas de Colombia. Ser. Publ. Esp. *Invenmar* 5, 176.
- Díaz-Pulido, G., and Garzón-Ferreira, J. (2002). Seasonality in algal assemblages on upwelling-influenced coral reefs in the Colombian caribbean. *Botanica Marina* 45, 284–292. doi: 10.1515/BOT.2002.028
- Dickson, A. G., Sabine, C. L., and Christian, J. R. eds. (2007). Guide to best practices for ocean CO₂ measurements. *PICES Special Publication* (Sidney, British Columbia: North Pacific Marine Science Organization). doi: 10.25607/OBP-1342
- Doney, S. C., Fabry, V. J., Feely, R. A., and Kleypas, J. A. (2009a). Ocean acidification: The other CO₂ problem. *Ann. Rev. Mar. Sci.* 1, 169–192. doi: 10.1146/annurev.marine.010908.163834
- Doney, S. C., Lima, I., Feely, R. A., Glover, D. M., Lindsay, K., Mahowald, N., et al. (2009b). Mechanisms governing interannual variability in upper-ocean inorganic carbon system and air–sea CO₂ fluxes: Physical climate and atmospheric dust. *Deep Sea Res. Part II: Topical Stud. Oceanography* 56, 640–655. doi: 10.1016/j.dsr2.2008.12.006
- Duarte, C. M., Hendriks, I. E., Moore, T. S., Olsen, Y. S., Steckbauer, A., Ramajo, L., et al. (2013). Is ocean acidification an open-ocean syndrome? Understanding anthropogenic impacts on seawater pH. *Estuaries Coasts* 36, 221–236. doi: 10.1007/s12237-013-9594-3
- Eidens, C., Bayraktarov, E., Hauffe, T., Pizarro, V., Wilke, T., and Wild, C. (2014). Benthic primary production in an upwelling-influenced coral reef, Colombian Caribbean. *PeerJ* 2014, e554. doi: 10.7717/peerj.554
- Emery, W. J., and Meincke, J. (1986). Global water masses-summary and review. *Oceanologica Acta* 9, 383–391.
- Fabry, V. J., Seibel, B. A., Feely, R. A., and Orr, J. C. (2008). Impacts of ocean acidification on marine fauna and ecosystem processes. *ICES J. Mar. Sci.* 65, 414–432. doi: 10.1093/icesjms/fsn048
- Feely, R. A., Boutin, J., Cosca, C. E., Dandonneau, Y., Etcheto, J., Inoue, H. Y., et al. (2002). Seasonal and interannual variability of CO₂ in the equatorial Pacific. *Deep Sea Res. Part II: Topical Stud. Oceanography* 49, 2443–2469. doi: 10.1016/S0967-0645(02)00044-9
- Feely, R. A., Okazaki, R. R., Cai, W.-J., Bednaršek, N., Alin, S. R., Byrne, R. H., et al. (2018). The combined effects of acidification and hypoxia on pH and aragonite saturation in the coastal waters of the California current ecosystem and the northern Gulf of Mexico. *Cont. Shelf Res.* 152, 50–60. doi: 10.1016/j.csr.2017.11.002
- Feely, R. A., Sabine, C. L., Hernandez-Ayon, J. M., Ianson, D., and Hales, B. (2008). Evidence for upwelling of corrosive "acidified" water onto the continental shelf. *Sci.* (1979) 320, 1490–1492. doi: 10.1126/science.1155676
- Feely, R. A., Sabine, C. L., Lee, K., Berelson, W., Kleypas, J., Fabry, V. J., et al. (2004). Impact of anthropogenic CO₂ on the CaCO₃ system in the oceans. *Sci.* (1979) 305, 362–366. doi: 10.1126/science.1097329
- Feely, R. A., Wanninkhof, R., Takahashi, T., and Tans, P. (1999). Influence of El Niño on the equatorial Pacific contribution to atmospheric CO₂ accumulation. *Nature* 398, 597–601. doi: 10.1038/19273
- Franco, A. C., Ianson, D., Ross, T., Hamme, R. C., Monahan, A. H., Christian, J. R., et al. (2021). Anthropogenic and climatic contributions to observed carbon system trends in the northeast Pacific. *Global Biogeochem Cycles* 35, e2020GB006829. doi: 10.1029/2020GB006829
- Gallego, M., Timmermann, A., Friedrich, T., and Zeebe, R. E. (2018). Drivers of future seasonal cycle changes in oceanic pCO₂. *Biogeosciences* 15, 5315–5327. doi: 10.5194/bg-15-5315-2018
- Garzón-Ferreira, J., Moreno-Bonilla, M., and Vásquez, J. M. V. (2004). Condición actual de las formaciones coralinas de acropora palmatay A. cervicornis en el Parque Nacional Natural Tayrona (Colombia). *Boletín Investigaciones Marinas y Costeras* 33, 117–136.
- Giraldo, L. (1994). Análisis de masas de agua y control de calidad de la información oceanográfica. *Boletín Científico C.L.O.H.* 15, 17–38. doi: 10.26640/22159045.71
- Gledhill, D. K., Wanninkhof, R., Millero, F. K., and Eakin, M. (2008). Ocean acidification of the greater caribbean region 1996–2006. *J. Geophys. Res. Oceans* 113, 1–11. doi: 10.1029/2007JC004629
- Good, S., Fiedler, E., Mao, C., Martin, M. J., Maycock, A., Reid, R., et al. (2020). The current configuration of the OSTIA system for operational production of foundation sea surface temperature and ice concentration analyses. *Remote Sens. (Basel)* 12, 720. doi: 10.3390/rs12040720
- Gregor, L., and Gruber, N. (2021). OceanSODA-ETHZ: a global gridded data set of the surface ocean carbonate system for seasonal to decadal studies of ocean acidification. *Earth Syst. Sci. Data* 13, 777–808. doi: 10.5194/essd-13-777-2021
- Guerrero, R., and Piola, A. R. (1997). Masas de agua en la plataforma continental. *El Mar. Argentino y sus recursos pesqueros* 1, 107–118.
- Gutiérrez, F., and Dracup, J. A. (2001). An analysis of the feasibility of long-range streamflow forecasting for Colombia using El Niño–Southern Oscillation indicators. *J. Hydrol. (Amst)* 246, 181–196. doi: 10.1016/S0022-1694(01)00373-0
- Hauri, C., Gruber, N., Vogt, M., Doney, S. C., Feely, R. A., Lachkar, Z., et al. (2013). Spatiotemporal variability and long-term trends of ocean acidification in the California Current System. *Biogeosciences* 10, 193–216. doi: 10.5194/bg-10-193-2013
- Hernández-Ayón, J. M., Chapa-Balcorta, C., Delgadillo-Hinojosa, F., Camacho-Ibar, V. F., Huerta-Díaz, M. A., Santamaria-del-Angel, E., et al. (2013). Dinámica del carbono inorgánico disuelto en la región de las grandes islas del golfo de California: Influencia de las masas de agua. *Cienc. Mar.* 39, 183–201. doi: 10.7773/cm.v39i2.2243
- Hernández-Ayón, J., Zirino, A., Marinone, S. G., Canino-Herrera, R., and Galindo-Bect, M. S. (2003). Relación pH-densidad en el agua de mar. *Cienc. Mar.* 29, 497–508. doi: 10.7773/cm.v29i4.166
- Hernandez-Guerra, A., and Joyce, T. M. (2000). Water masses and circulation in the surface layers of the Caribbean at 66°W. *Geophys. Res. Lett.* 27, 3497–3500. doi: 10.1029/1999GL011230
- Herrera-Fajardo, S., Bastidas-Salamanca, M., and Ordóñez-Zúñiga, A. (2017). “Región 5: la guajira-tayrona,” in *Regionalización oceanográfica: una visión dinámica del Caribe*. Eds. C. Ricaurte-Villota and M. L. Bastidas-Salamanca (Invenmar, Santa Marta), 94–105.
- Hersbach, H., Bell, B., Berrisford, P., Biavati, G., Horányi, A., Muñoz Sabater, J., et al. (2023). ERA5 monthly averaged data on single levels from 1940 to present [Dataset] (Copernicus Climate Change Service (C3S) Climate Data Store (CDS)).
- Hofmann, G. E., Smith, J. E., Johnson, K. S., Send, U., Levin, L. A., Micheli, F., et al. (2011). High-frequency dynamics of ocean pH: a multi-ecosystem comparison. *PLoS One* 6, e28983. doi: 10.1371/journal.pone.0028983
- Ibáñez, J. S. P., Diverrès, D., Araujo, M., and Lefèvre, N. (2015). Seasonal and interannual variability of sea-air CO₂ fluxes in the tropical Atlantic affected by the Amazon River plume. *Global Biogeochem Cycles* 29, 1640–1655. doi: 10.1002/2015GB005110
- Johnson, K. M., Sieburth, J. M., leB Williams, P. J., and Brändström, L. (1987). Coulometric total carbon dioxide analysis for marine studies: automation and calibration. *Mar. Chem.* 21 (2), 117–133.
- Lan, X., Mund, J. W., Crotwell, A. M., Crotwell, M. J., Moglia, E., Madronich, M. (2024). Atmospheric carbon dioxide dry air mole fractions from the NOAA GML carbon cycle cooperative global air sampling network, 1968–2022. Version: 2023-08-28. doi: 10.15138/wkji-f215
- Lefèvre, N., Mejía, C., Khvorostyanov, D., Beaumont, L., and Koffi, U. (2021). Ocean circulation drives the variability of the carbon system in the eastern tropical atlantic. *Oceans-switzerland* 2, 126–148. doi: 10.3390/OCEANS2010008
- Lefèvre, N., Urbano, D. F., Gallois, F., and Diverrès, D. (2014). Impact of physical processes on the seasonal distribution of the fugacity of CO₂ in the western tropical Atlantic. *J. Geophys. Res. Oceans* 119, 646–663. doi: 10.1002/2013JC009248
- Lewis, E., Wallace, D., and Allison, L. J. (1998). Program developed for CO₂ {sub 2} system calculations (No. ORNL/CDIAC-105). *Brookhaven National Lab., Dept. of Applied Science* (Upton, NY (United States): Oak Ridge National Lab., Carbon Dioxide Information Analysis Center, TN (United States)).
- Liu, B., Tan, X., Gan, T. Y., Chen, X., Lin, K., Lu, M., et al. (2020). Global atmospheric moisture transport associated with precipitation extremes: Mechanisms and climate change impacts. *Wiley Interdiscip. Reviews: Water* 7, e1412. doi: 10.1002/wat2.1412
- Lovenduski, N. S., Gruber, N., Doney, S. C., and Lima, I. D. (2007). Enhanced CO₂ outgassing in the Southern Ocean from a positive phase of the Southern Annular Mode. *Global Biogeochem Cycles* 21, 2026. doi: 10.1029/2006GB002900
- Manzello, D. P., Enochs, I. C., Bruckner, A., Renaud, P. G., Kolodziej, G., Budd, D. A., et al. (2014). Galápagos coral reef persistence after ENSO warming across an acidification gradient. *Geophys. Res. Lett.* 41, 9001–9008. doi: 10.1002/2014GL062501.Received
- Millero, F. J. (2010). Carbonate constants for estuarine waters. *Mar. Freshw. Res.* 61, 139–142. doi: 10.1071/MF09254
- Miloslavich, P., Díaz, J. M., Klein, E., Alvarado, J. J., Díaz, C., Gobin, J., et al. (2010). Marine biodiversity in the caribbean: Regional estimates and distribution patterns. *PLoS One* 5, e11916. doi: 10.1371/journal.pone.0011916
- Montoya-Sánchez, R. A., Devis-Morales, A., Bernal, G., and Poveda, G. (2018). Seasonal and intraseasonal variability of active and quiescent upwelling events in the Guajira system, southern Caribbean Sea. *Cont. Shelf Res.* 171, 97–112. doi: 10.1016/j.csr.2018.10.006
- Norzagaray-López, O., Ávila-López, M., del, C., Chapa-Balcorta, C., Luis, C.-A., and Hernández-Ayón, M. (2013). Reducida producción de CaCO₃ por *Porites panamensis* en tres comunidades arrecifales del Pacífico mexicano *Síntesis* a. 437–441.
- Norzagaray-López, C. O., Calderon-Aguilera, L. E., Hernández-Ayón, J. M., Reyes-Bonilla, H., Carricart-Ganivet, J. P., Cabral-Tena, R. A., et al. (2015). Low calcification rates and calcium carbonate production in *Porites panamensis* at its northernmost geographic distribution. *Mar. Ecol.* 36, 1244–1255. doi: 10.1111/maec.12227
- Norzagaray-López, C. O., Hernández-Ayón, J. M., Calderon-Aguilera, L. E., Reyes-Bonilla, H., Chapa-Balcorta, C., and Ayala-Bocos, A. (2017). Aragonite saturation and pH variation in a fringing reef are strongly influenced by oceanic conditions. *Limnol Oceanogr* 62, 2375–2388. doi: 10.1002/lno.10571
- Omar, A. M., Thomas, H., Olsen, A., Becker, M., Skjelvan, I., and Reverdin, G. (2019). Trends of ocean acidification and pCO₂ in the northern North Sea, 2003–2015. *J. Geophys. Res.: Biogeosci.* 124 (10), 3088–3103.
- Orr, J. C., Epitalon, J.-M., Dickson, A. G., and Gattuso, J.-P. (2018). Routine uncertainty propagation for the marine carbon dioxide system. *Mar. Chem.* 207, 84–107. doi: 10.1016/j.marchem.2018.10.006
- Orr, J. C., Fabry, V. J., Aumont, O., Bopp, L., Doney, S. C., Feely, R. A., et al. (2005). Anthropogenic ocean acidification over the twenty-first century and its impact on calcifying organisms. *Nature* 437, 681–686. doi: 10.1038/nature04095

- Parard, G., Lefèvre, N., and Boutin, J. (2010). Sea water fugacity of CO₂ at the PIRATA mooring at 6 S, 10 W. *Tellus B: Chem. Phys. Meteorology* 62, 636–648. doi: 10.1111/j.1600-0889.2010.00503.x
- Poveda, G., and Mesa, O. J. (1996). Las fases extremas del fenómeno ENSO (El Niño y La Niña) y su influencia sobre la hidrología de Colombia. *Tecnología y Cienc. del agua* 11, 21–37.
- Poveda, G., and Mesa, O. J. (1997). Feedbacks between hydrological processes in tropical South America and large-scale ocean-atmospheric phenomena. *J. Clim* 10, 2690–2702. doi: 10.1175/1520-0442(1997)010<2690:FBHPIT>2.0.CO;2
- Pujos, M., Pagliardini, J.-L., Steer, R., Vernet, G., and Oliver, W. (1986). Influencia de la contracorriente norte colombiana para la circulación de las aguas en la plataforma continental su acción sobre la dispersión de los efluentes en suspensión del Río Magdalena. *Boletín científico CIOH* 6, 3–15. doi: 10.26640/01200542.6.3_15
- Restrepo, J. D., and Kjerfve, B. (2000). Magdalena river: interannual variability (1975–1995) and revised water discharge and sediment load estimates. *J. Hydrol. (Amst.)* 235, 137–149. doi: 10.1016/S0022-1694(00)00269-9
- Restrepo, J. D., Zapata, P., Díaz, J. M., Garzón-Ferreira, J., and García, C. B. (2006). Fluvial fluxes into the Caribbean Sea and their impact on coastal ecosystems: The Magdalena River, Related papers. *Glob Planet Change* 50, 33–49. doi: 10.1016/j.gloplacha.2005.09.002
- Rheuban, J. E., Doney, S. C., McCorkle, D. C., and Jakuba, R. W. (2019). Quantifying the effects of nutrient enrichment and freshwater mixing on coastal ocean acidification. *J. Geophys. Res. Oceans* 124, 9085–9100. doi: 10.1029/2019JC015556
- Ricaurte-Villota, C., Bastidas-Salamanca, M., Caicedo Carrascal, F. M., and Arbeláez Salazar, J. D. (2018). Estudio integral de la Ciénaga Grande de Santa Marta -Fase II(B): modelaciones hidráulica, hidrosedimentológica y biogeoquímica. Instituto de Investigaciones Marinas y Costeras “José Benito Vives de Andreis” - INVEMAR & Corporación Autónoma Regional del Magdalena - CORPAMAG. 72 p.
- Romero-Rodríguez, D. A., Peña-Mejía, C., Ordóñez-Zuñiga, A., Ricaurte-Villota, C., and Bastidas-Salamanca, M. L. (2017). “Región 6: Ciénaga Grande de Santa Marta, río Magdalena, Bolívar.” in *Regionalización oceanográfica: una visión dinámica del Caribe*. Eds. C. Ricaurte-Villota and M. L. Bastidas-Salamanca (Instituto de Investigaciones Marinas y Costeras José Benito Vives De Andreis (INVEMAR, Santa Marta), 106–123.
- Rueda-Roa, D. T., and Muller-Karger, F. E. (2013). The southern Caribbean upwelling system: Sea surface temperature, wind forcing and chlorophyll concentration patterns. *Deep Sea Res. 1 Oceanogr Res. Pap* 78, 102–114. doi: 10.1016/j.dsr.2013.04.008
- Sabine, C. L., and Feely, R. A. (2007). The oceanic sink for carbon dioxide. *Chapter 3 In Greenhouse Gas Sinks*, D. Reay, N. Hewitt, J. Grace and K. Smith (eds.), (Oxfordshire, UK: CABI Publishing), 31–49.
- Salisbury, J., Vandemark, D., Hunt, C., Campbell, J., Jonsson, B., Mahadevan, A., et al. (2009). Episodic riverine influence on surface DIC in the coastal Gulf of Maine. *Estuar. Coast. Shelf Sci.* 82, 108–118. doi: 10.1016/j.ecss.2008.12.021
- Salzwedel, H., and Müller, K. (1983). A summary of meteorological and hydrological data from the bay of Santa Marta, Colombian Caribbean. *Anales Instituto Investigación Marina Punta Betín* 13, 67–83.
- Sánchez-Noguera, C., Stuhldreier, I., Cortés, J., Jiménez, C., Morales, Á., Wild, C., et al. (2018). Natural ocean acidification at Papagayo upwelling system (north Pacific Costa Rica): Implications for reef development. *Biogeosciences* 15, 2349–2360. doi: 10.5194/bg-15-2349-2018
- Sarmiento-Devía, R. A., López-Escobar, Á.V., Mejías, M. B., Dávila, P. M., and Franco-Herrera, A. (2013). Intra-annual variation of climate regime on upwelling zones in the Southeast Caribbean Sea. *Rev. Biol. Mar. Oceanogr* 48, 471–485. doi: 10.4067/s0718-19572013000300006
- Silverman, J., Lazar, B., Cao, L., Caldeira, K., and Erez, J. (2009). Coral reefs may start dissolving when atmospheric CO₂ doubles. *Geophys. Res. Lett.* 36, 1–5. doi: 10.1029/2008GL036282
- Takahashi, T., Sutherland, S. C., Chipman, D. W., Goddard, J. G., and Ho, C. (2014). Climatological distributions of pH, pCO₂, total CO₂, alkalinity, and CaCO₃ saturation in the global surface ocean, and temporal changes at selected locations. *Mar. Chem.* 164, 95–125. doi: 10.1016/j.marchem.2014.06.004
- Takahashi, T., Sutherland, S. C., Sweeney, C., Poisson, A., Metzl, N., Tilbrook, B., et al. (2002). Global sea-air CO₂ flux based on climatological surface ocean pCO₂, and seasonal biological and temperature effects. *Deep Sea Res. Part II: Topical Stud. Oceanography* 49, 1601–1622. doi: 10.1016/S0967-0645(02)00003-6
- Takahashi, T., Sutherland, S. C., Wanninkhof, R., Sweeney, C., Feely, R. A., Chipman, D. W., et al. (2009). Climatological mean and decadal change in surface ocean pCO₂, and net sea-air CO₂ flux over the global oceans. *Deep Sea Res. 2 Top. Stud. Oceanogr* 56, 554–577. doi: 10.1016/j.dsr2.2008.12.009
- Tigreros, P. C. (2013). *La dinámica del CO₂ en el Caribe centro-norte Colombiano y su efecto sobre la comunidad fitoplanctónica* (Colombia: Fundación Universidad de Bogotá Jorge Tadeo Lozano).
- Tomczak, M. (1999). Some historical, theoretical and applied aspects of quantitative water mass analysis. *J. Mar. Res.* 57, 275–303. doi: 10.1357/002224099321618227
- Trenberth, K. E. (1998). Atmospheric moisture residence times and cycling: Implications for rainfall rates and climate change. *Clim Change* 39, 667–694. doi: 10.1023/A:1005319109110
- Turi, G., Lachkar, Z., Gruber, N., and Münnich, M. (2016). Climatic modulation of recent trends in ocean acidification in the California Current System. *Environ. Res. Lett.* 11, 014007. doi: 10.1088/1748-9326/11/1/014007
- Valerio, A. M., Kampel, M., Ward, N. D., Sawakuchi, H. O., Cunha, A. C., and Richey, J. E. (2021). CO₂ partial pressure and fluxes in the Amazon River plume using *in situ* and remote sensing data. *Cont Shelf Res.* 215, 104348. doi: 10.1016/j.csr.2021.104348
- Waldbusser, G. G., Hales, B., and Haley, B. A. (2016). Calcium carbonate saturation state: on myths and this or that stories. *ICES J. Mar. Sci.* 73, 563–568. doi: 10.1093/icesjms/fsv174
- Waldbusser, G. G., and Salisbury, J. E. (2014). Ocean acidification in the coastal zone from an organism's perspective: Multiple system parameters, frequency domains, and habitats. *Ann. Rev. Mar. Sci.* 6, 221–247. doi: 10.1146/annurev-marine-121211-172238
- Wang, D., Gouhier, T. C., Menge, B. A., and Ganguly, A. R. (2015). Intensification and spatial homogenization of coastal upwelling under climate change. *Nature* 518, 390–394. doi: 10.1038/nature14235
- Wang, G., and Schimel, D. (2003). Climate change, climate modes, and climate impacts. *Annu. Rev. Environ. Resour* 28, 1–28. doi: 10.1146/annurev.energy.28.050302.105444
- Wanninkhof, R. (1992). Relationship between wind speed and gas exchange over the ocean. *J. Geophys. Res. Oceans* 97, 7373–7382. doi: 10.1029/92JC00188
- Wanninkhof, R. (2014). Relationship between wind speed and gas exchange over the ocean revisited. *Limnol Oceanogr Methods* 12, 351–362. doi: 10.4319/lom.2014.12.351
- Wanninkhof, R., Pierrot, D., Sullivan, K., Barbero, L., and Triñanes, J. (2020). A 17-year dataset of surface water fugacity of CO₂ along with calculated pH, aragonite saturation state and air-sea CO₂ fluxes in the northern Caribbean Sea. *Earth Syst. Sci. Data* 12, 1489–1509. doi: 10.5194/ESSD-12-1489-2020
- Weiss, R. (1974). Carbon dioxide in water and seawater: the solubility of a non-ideal gas. *Mar. Chem.* 2, 203–215. doi: 10.1016/0304-4203(74)90015-2
- Woosley, R. J., Millero, F. J., and Wanninkhof, R. (2016). Rapid anthropogenic changes in CO₂ and pH in the Atlantic Ocean: 2003–2014. *Global Biogeochem Cycles* 30, 70–90. doi: 10.1002/2015GB005248.Received
- Wright-Fairbanks, E. K., and Saba, G. K. (2022). Quantification of the dominant drivers of acidification in the coastal mid-atlantic bight. *J. Geophys. Res. Oceans* 127, e2022JC018833. doi: 10.1029/2022JC018833
- Zeebe, R. E., and Wolf-Gladrow, D. (2001). *CO₂ in seawater: equilibrium, kinetics, isotopes*. (Gulf Professional Publishing). 65, 346.